Analysis and measurement of anti-reciprocal systems

Noori Kim (Advisor: Jont B. Allen)
Human Speech Recognition group

Nov 7, 2014

Thesis objective:

- Provide a clear insight into "Anti-reciprocal" systems such as electromagnetic systems

Thesis contents

1. INTRODUCTION
2. THEORETICAL METHODS
3. EXPERIMENTAL METHODS
4. RESULTS
5. CONCLUSIONS and CONTRIBUTIONS

Major updates after my preliminary exam….

1. Using a conceptual BAR model, I linked all subtopics of my thesis into one place to strengthen and organize my thesis structure

Projecting thesis topics onto the transducer model

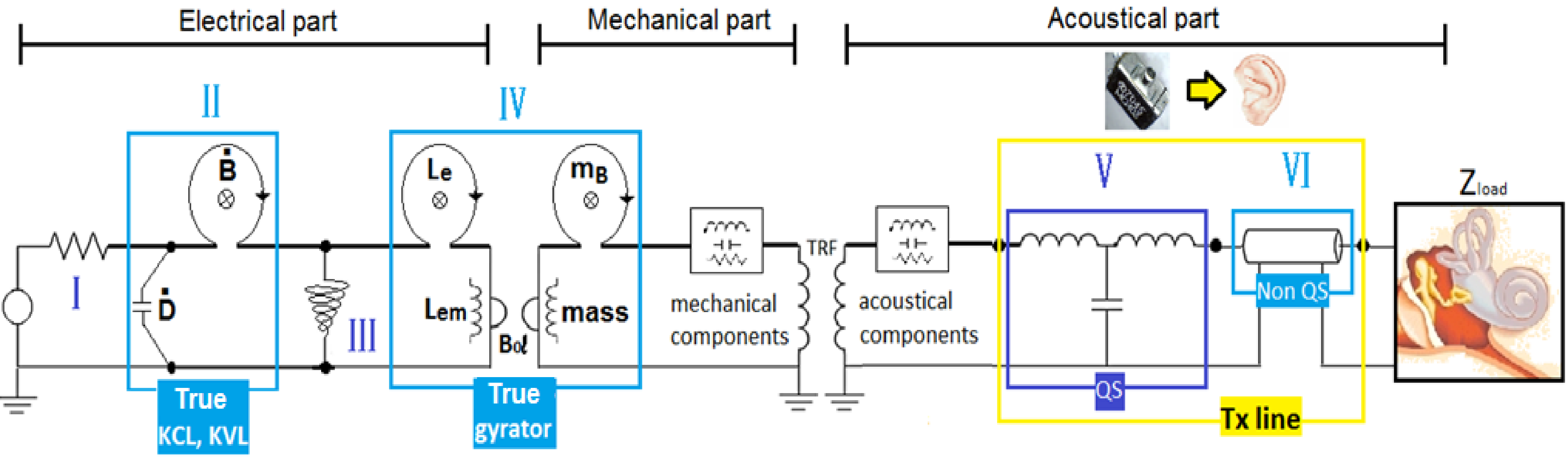

Thesis contents

1. INTRODUCTION
2. THEORETICAL METHODS
3. EXPERIMENTAL METHODS
4. RESULTS
5. CONCLUSIONS and CONTRIBUTIONS

Theory part

Experimental and application part

Major updates after my preliminary exam….

1. Using a conceptual BAR model, I linked all subtopics of my thesis into one place to strengthen and organize my thesis structure

2. I added more experimental work and result, such as hearing measurement probe manufacturing procedure.

I. Theoretical part

- I take a Balanced Armature Receiver (BAR, a speaker used in hearing-aids) as a specific example of the "Anti-reciprocal" system to demonstrate the system's operational principle

II. Experimental part

- I introduce
  - Experiments to support (verify) my theory
  - An example to make use of the BAR; the hearing measurement probe manufacturing

I. Theoretical part

- **An answer for the question: how does the BAR work?**
  - **Introduction of BAR**
  - **Overview of BAR's operational principle**
  - **Case study I=0 and I≠0 (Eddy-currents)**
  - **Force on the armature (F_m) with Hysteresis effect**

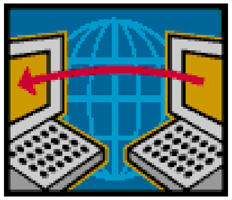

During my talk, I will bring up my conceptual model if the slide is relevant to explain each section in the model.

Balanced Armature Receiver (BAR)

- The oldest telephone receiver was invented by A. G. Bell in 1876

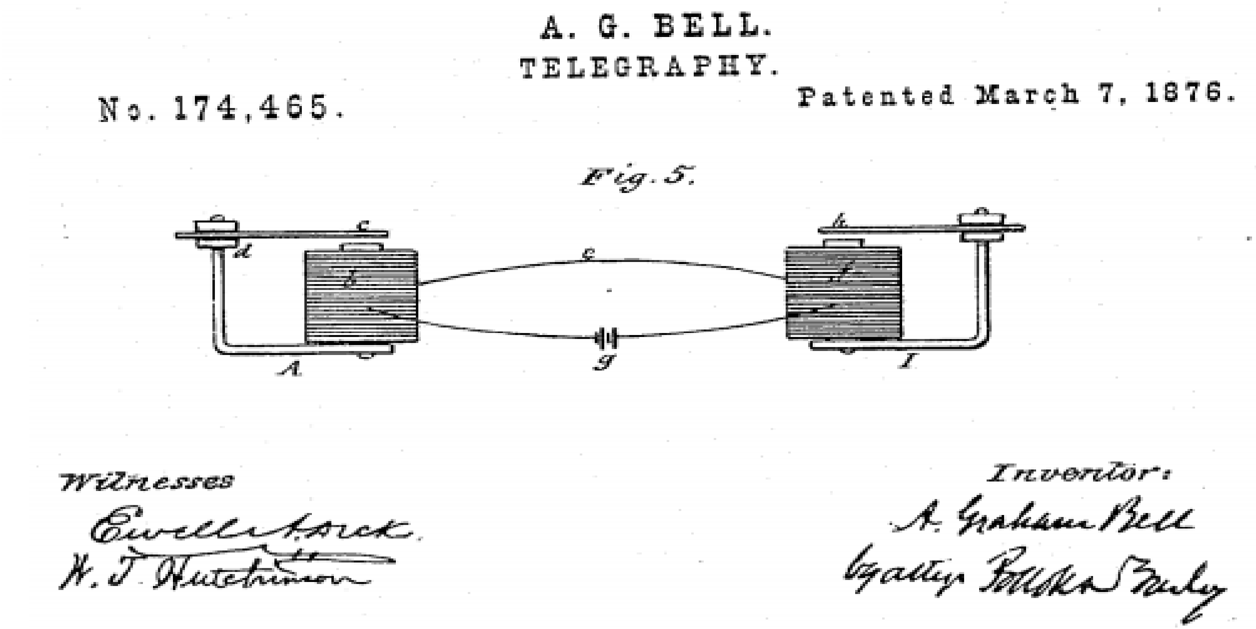

- Attraction and release of the armature are controlled by the current from the coils, which generates electromagnetic fields
- It has evolved into the modern hearing-aid devices

An example of the modern style BAR, Knowles ED7045

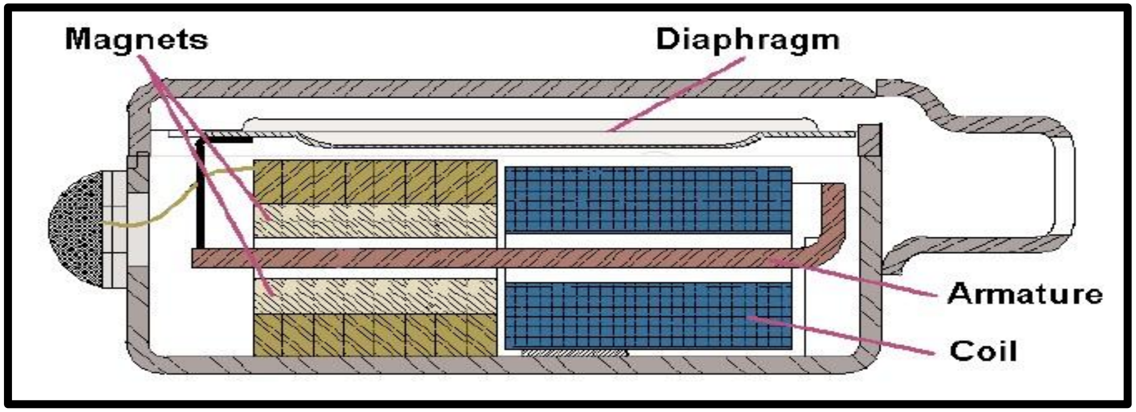

Cross section of Knowles ED receiver

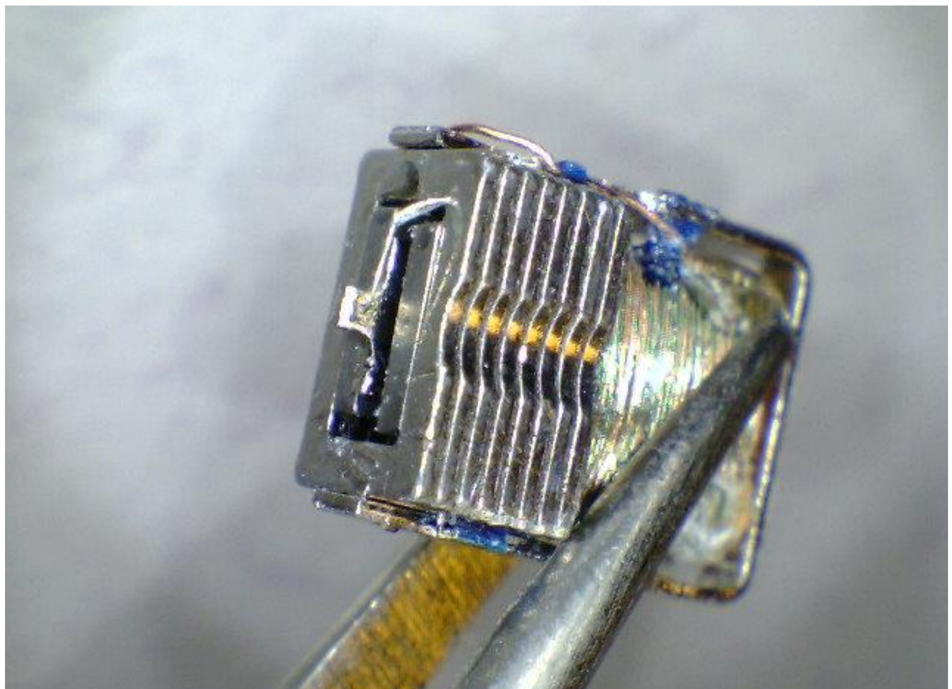

Inside of the BAR without case and diaphragm

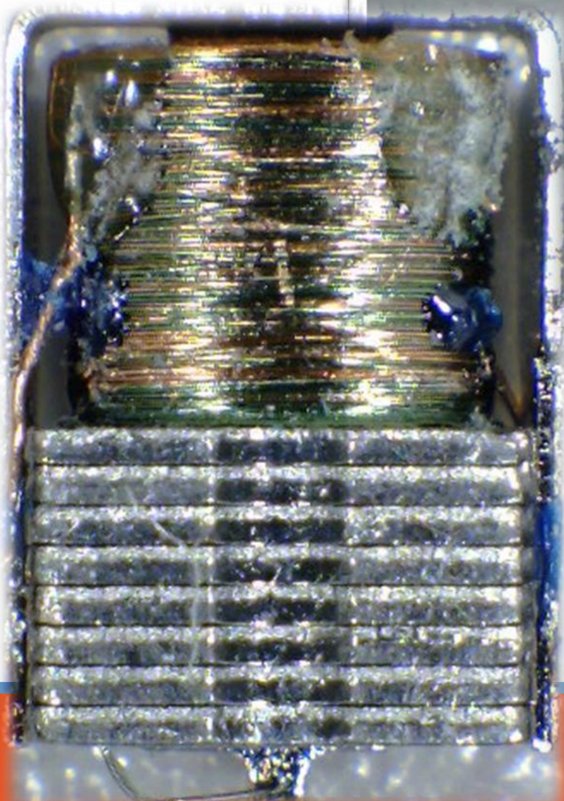

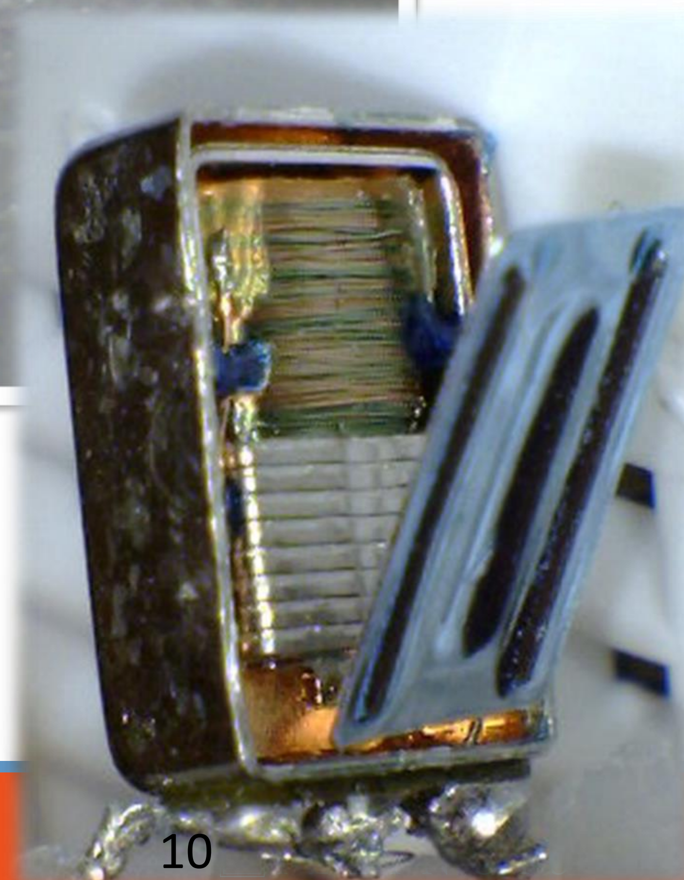

Overview of the BAR's operation

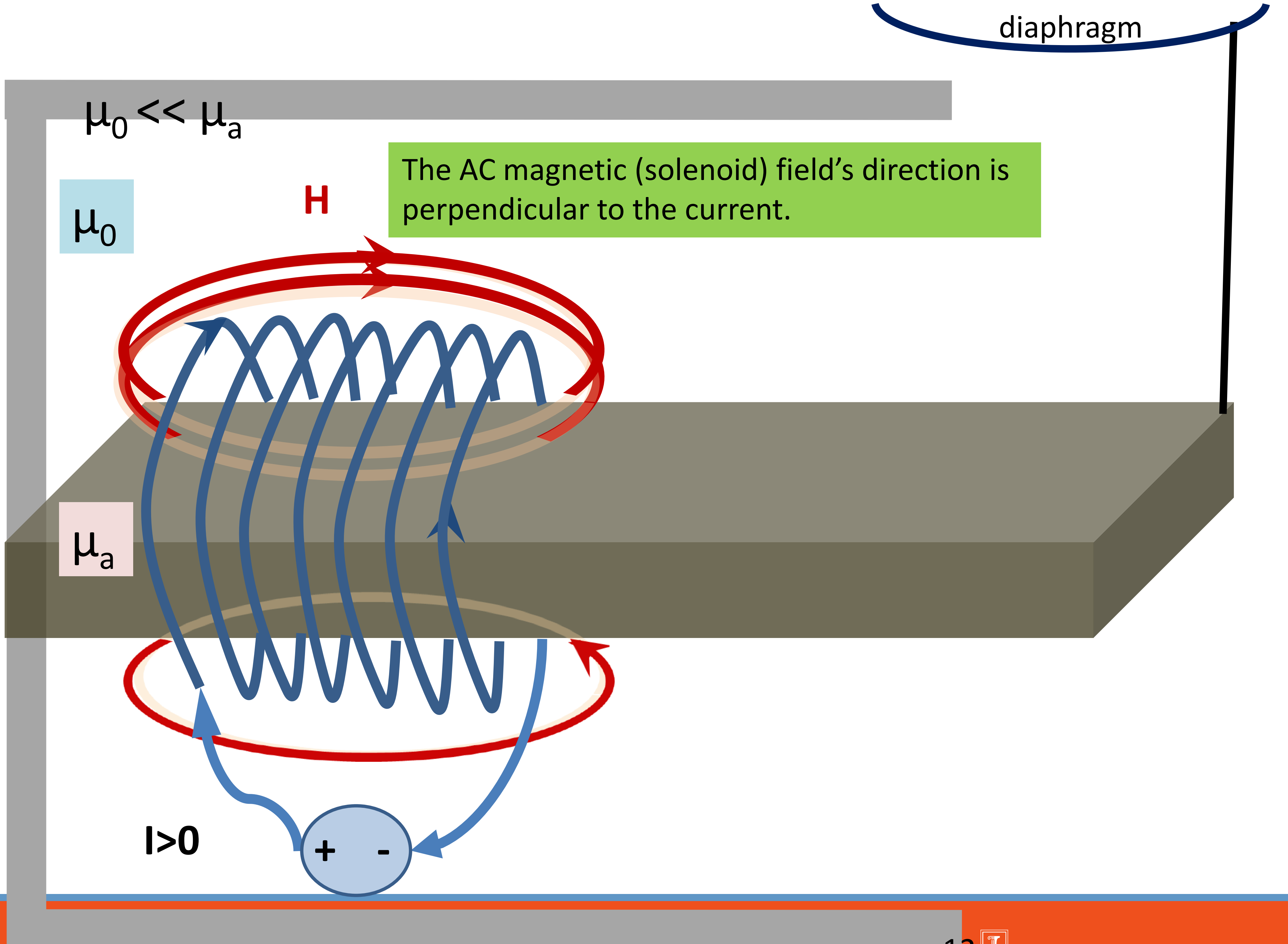

The AC magnetic (solenoid) field's direction is perpendicular to the current.

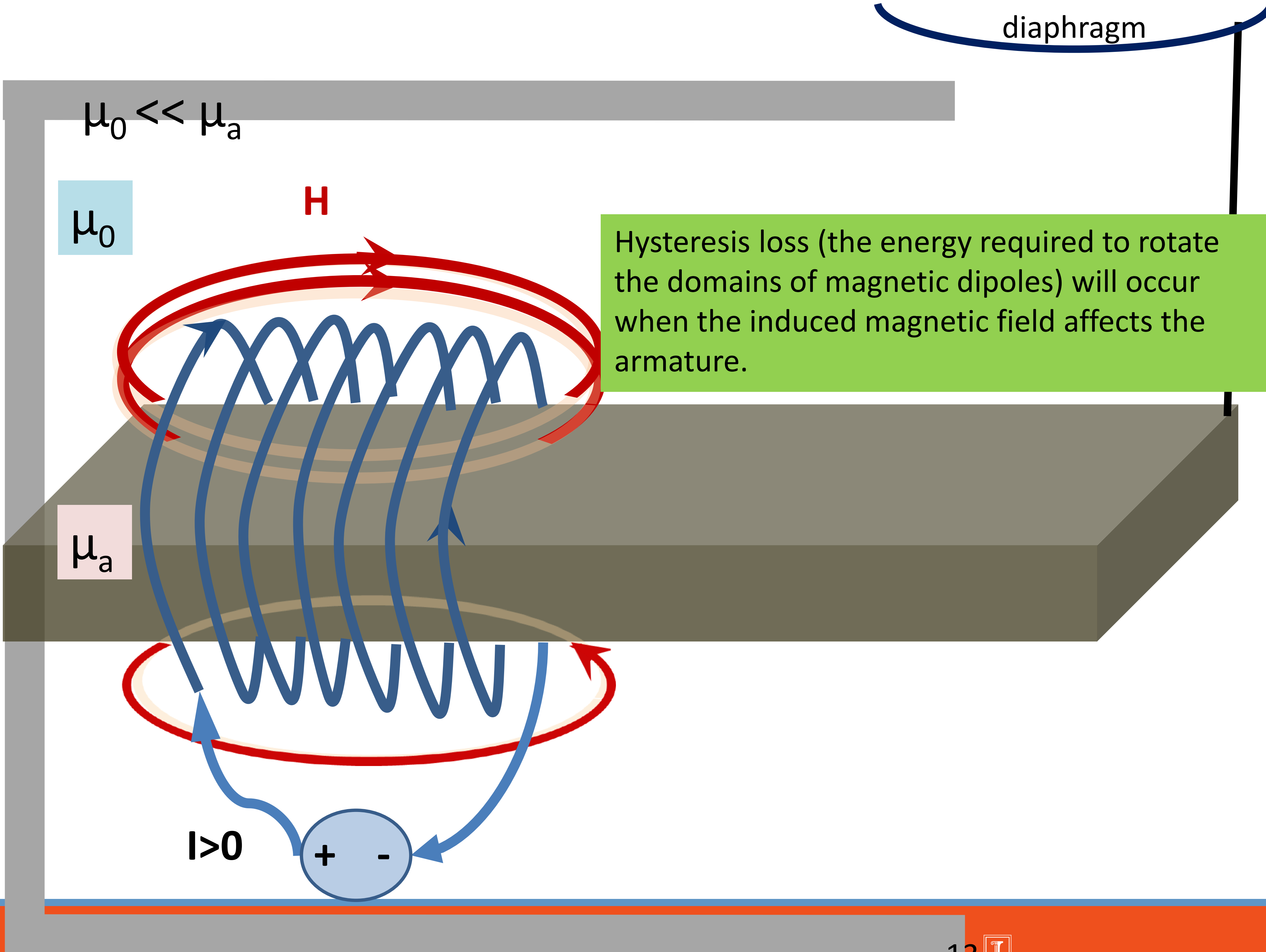

Hysteresis loss (the energy required to rotate the domains of magnetic dipoles) will occur when the induced magnetic field affects the armature.

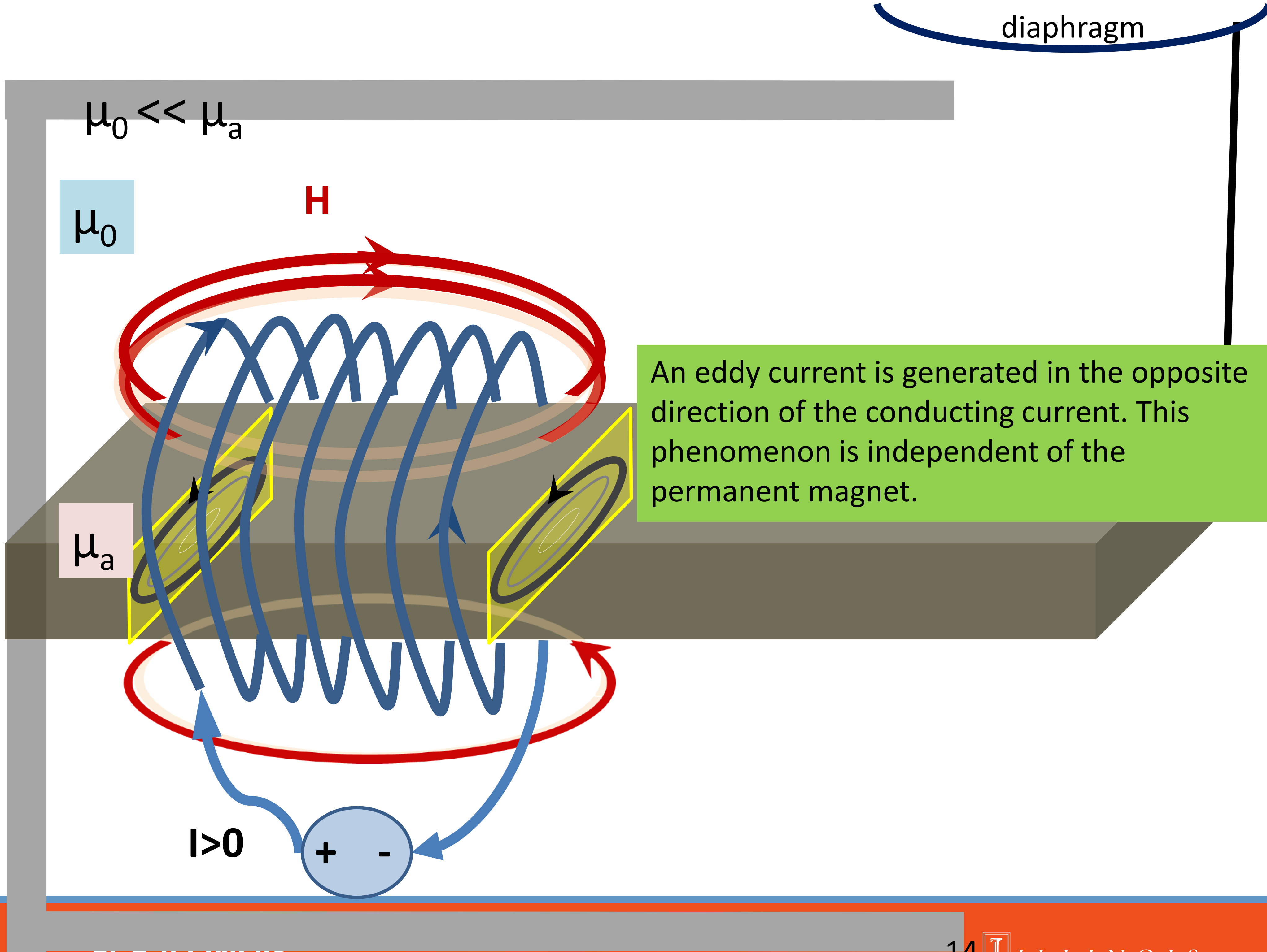

An eddy current is generated in the opposite direction of the conducting current. This phenomenon is independent of the permanent magnet.

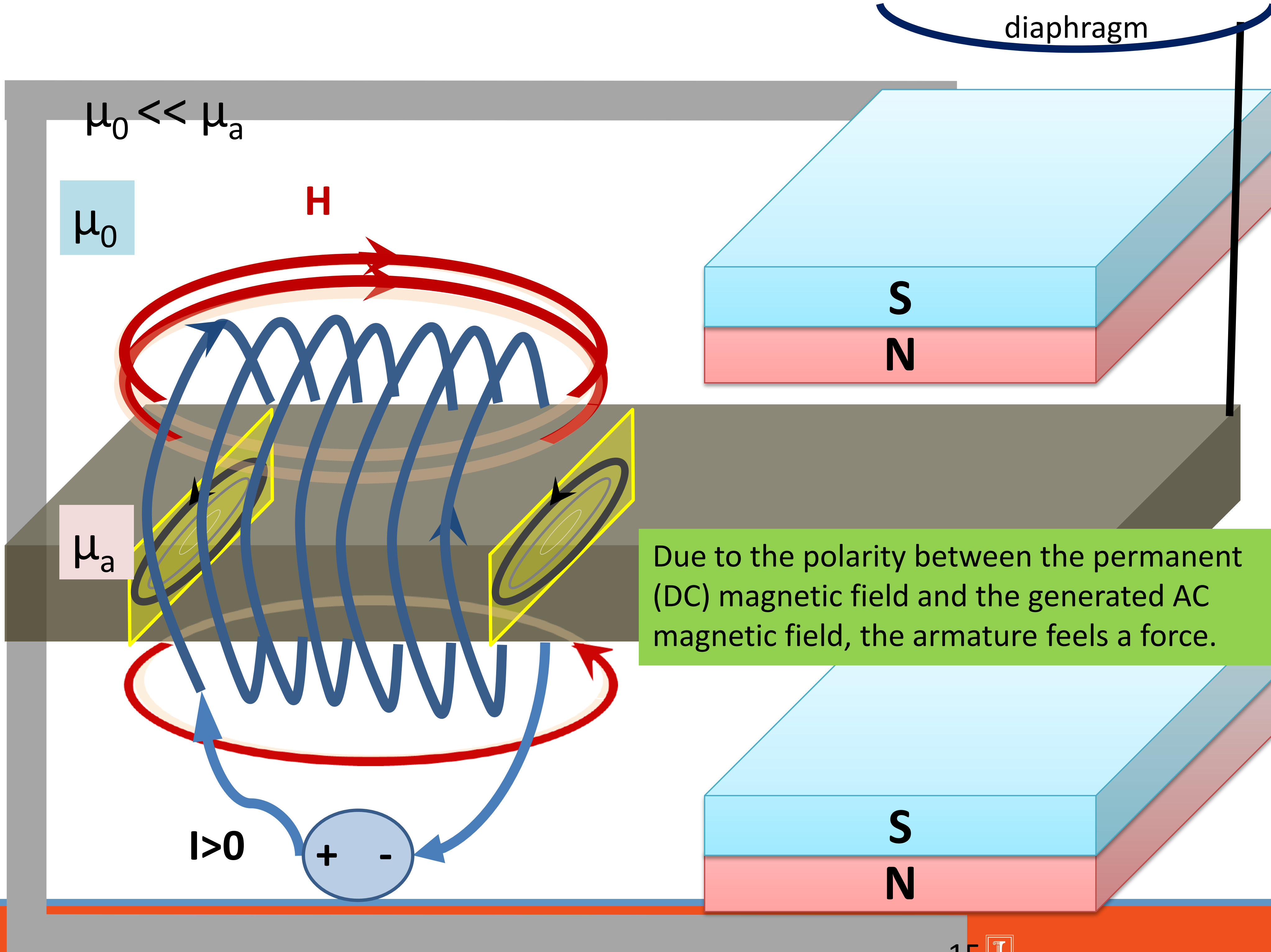

Due to the polarity between the permanent (DC) magnetic field and the generated AC magnetic field, the armature feels a force.

Magnetic force, F_m: Force between two nearby magnetized surfaces to create a magnetic image

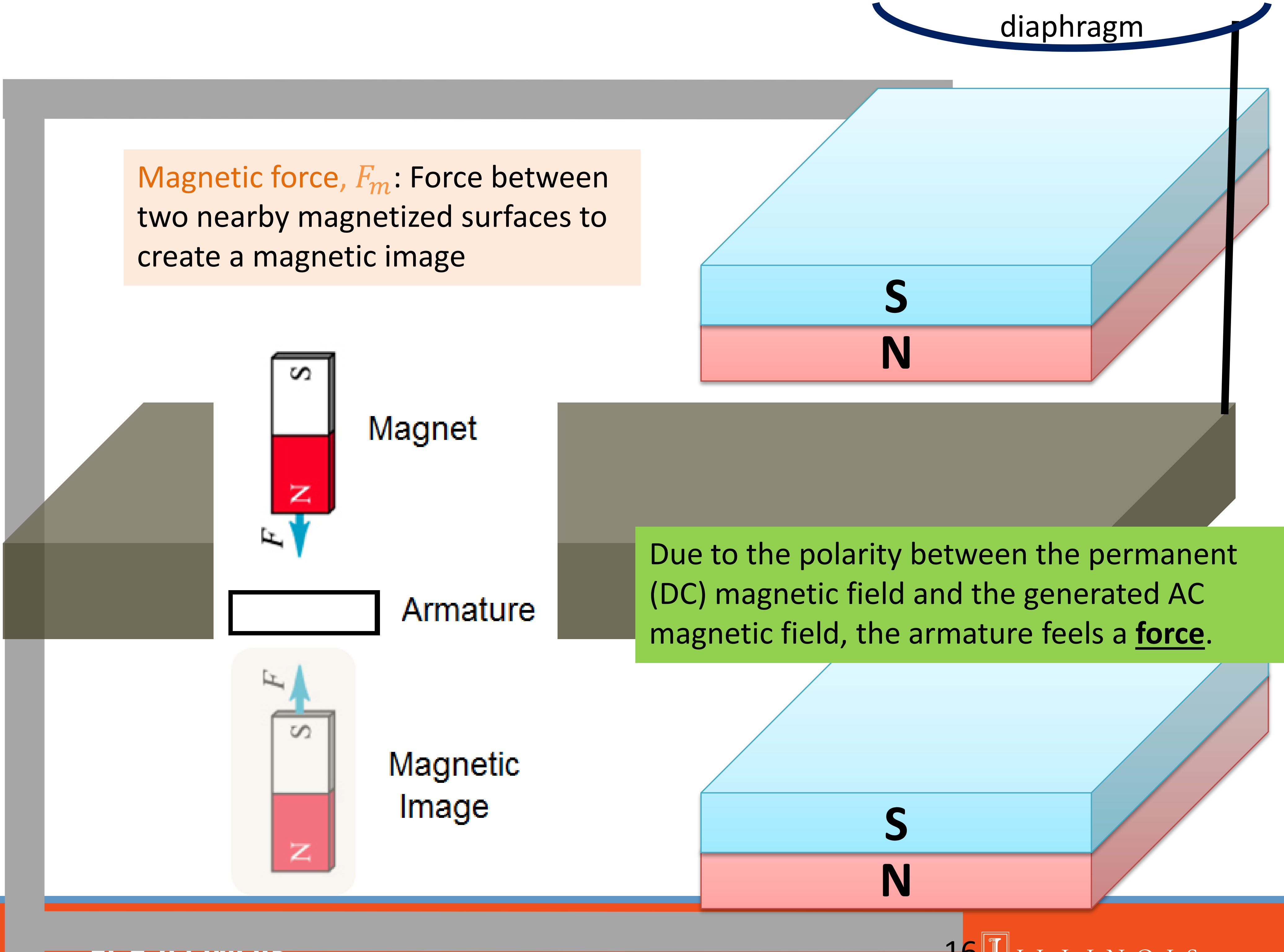

Due to the polarity between the permanent (DC) magnetic field and the generated AC magnetic field, the armature feels a **force**.

The BAR's behavior:

$\mathrm{I} = 0$ and $\mathrm{I} \neq 0$ (Eddy-currents)

I=0

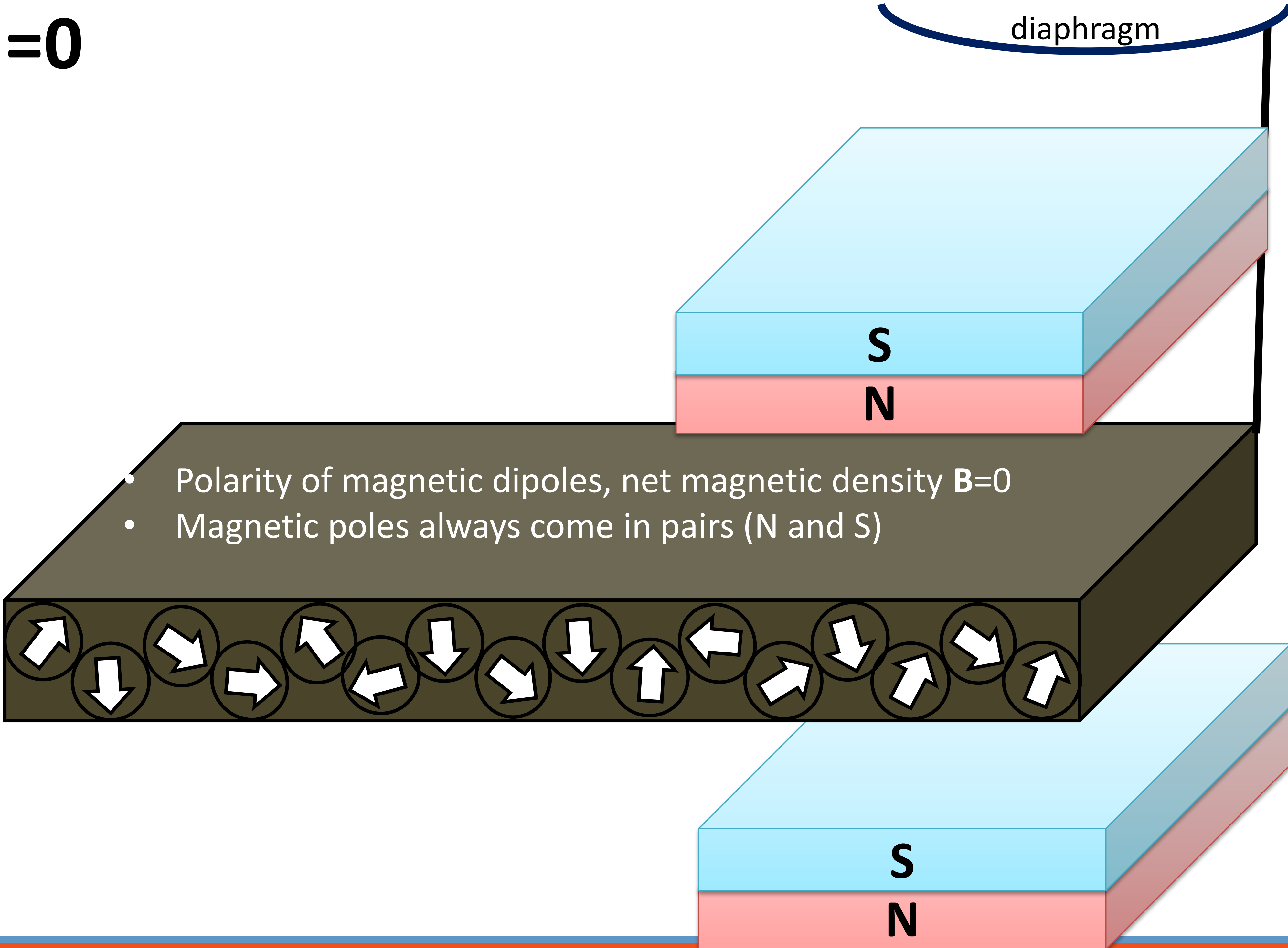

- Polarity of magnetic dipoles, net magnetic density **B**=0
- Magnetic poles always come in pairs (N and S)

I=0

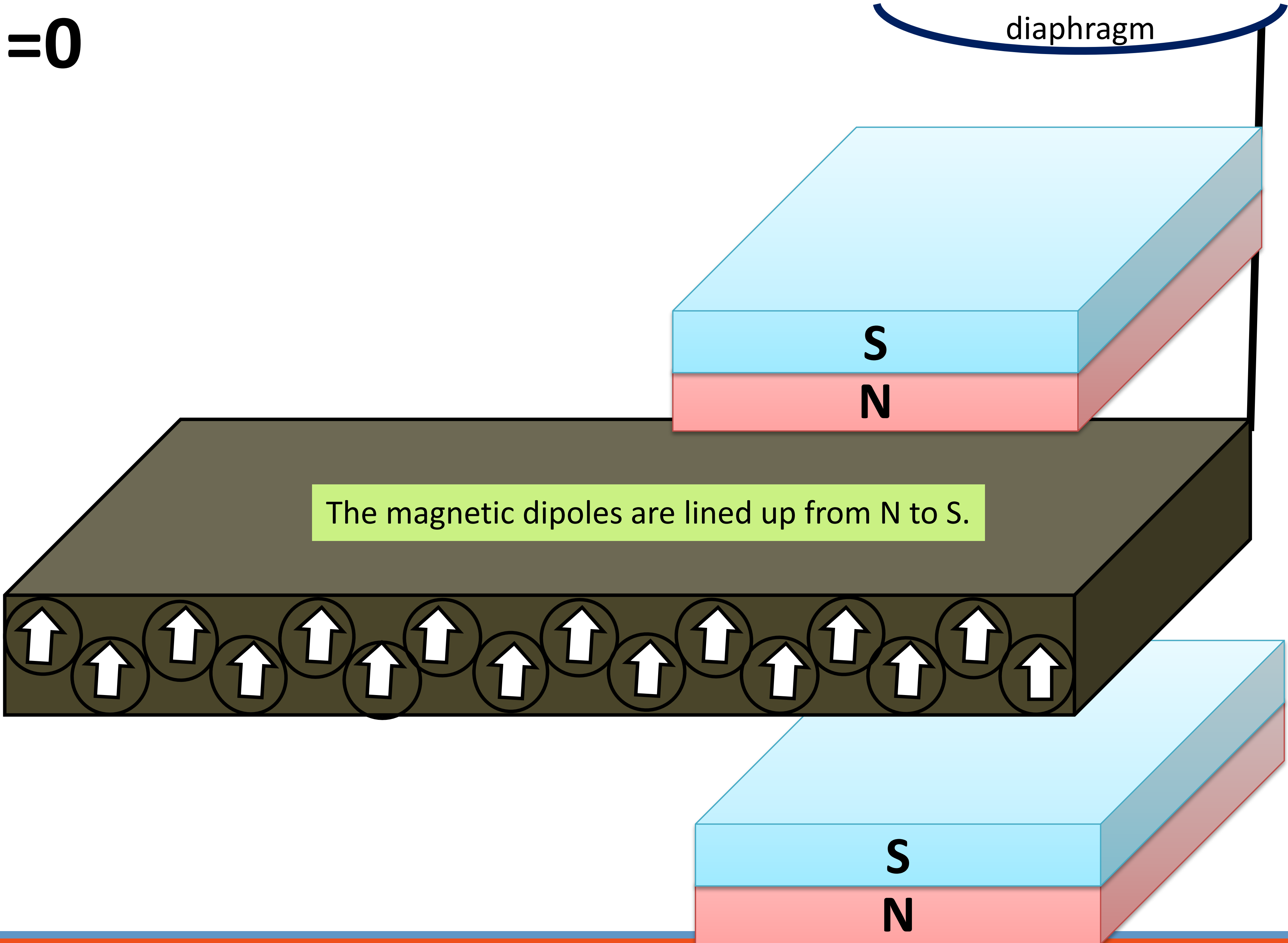

I=0

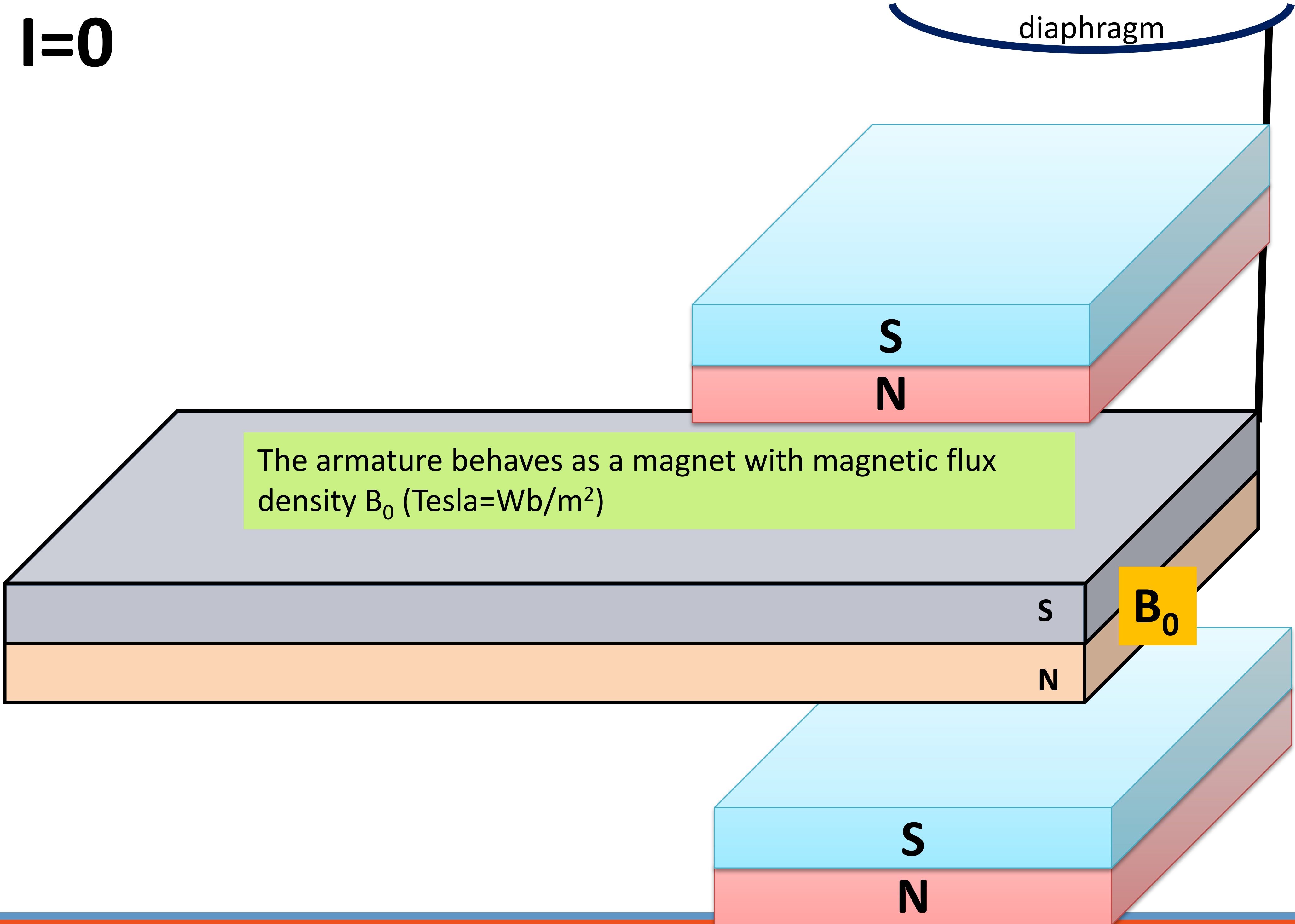

diaphragm
S
N
The armature behaves as a magnet with magnetic flux density B_0 (Tesla=Wb/m^2)
S
N
B_0
S
N

I=0

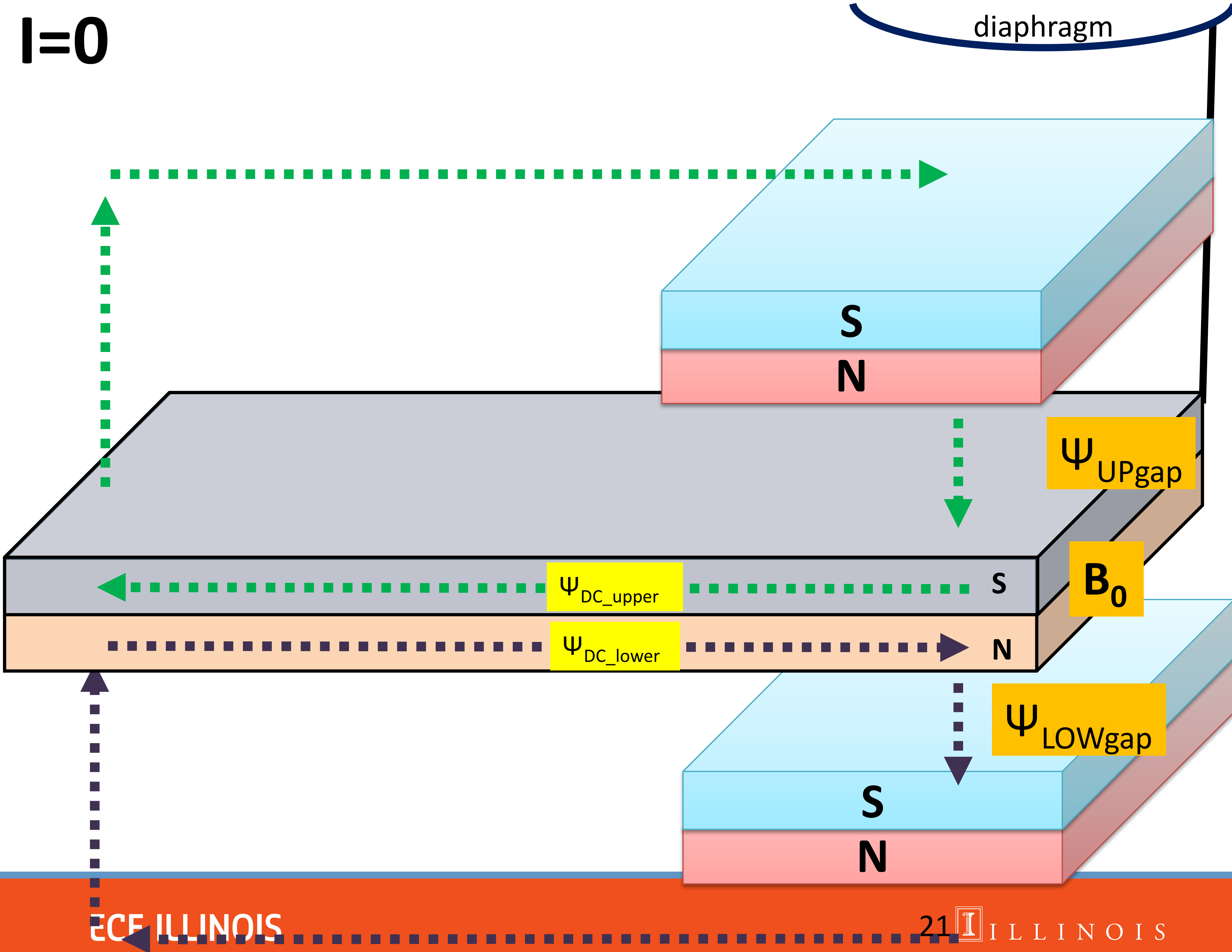

I=0

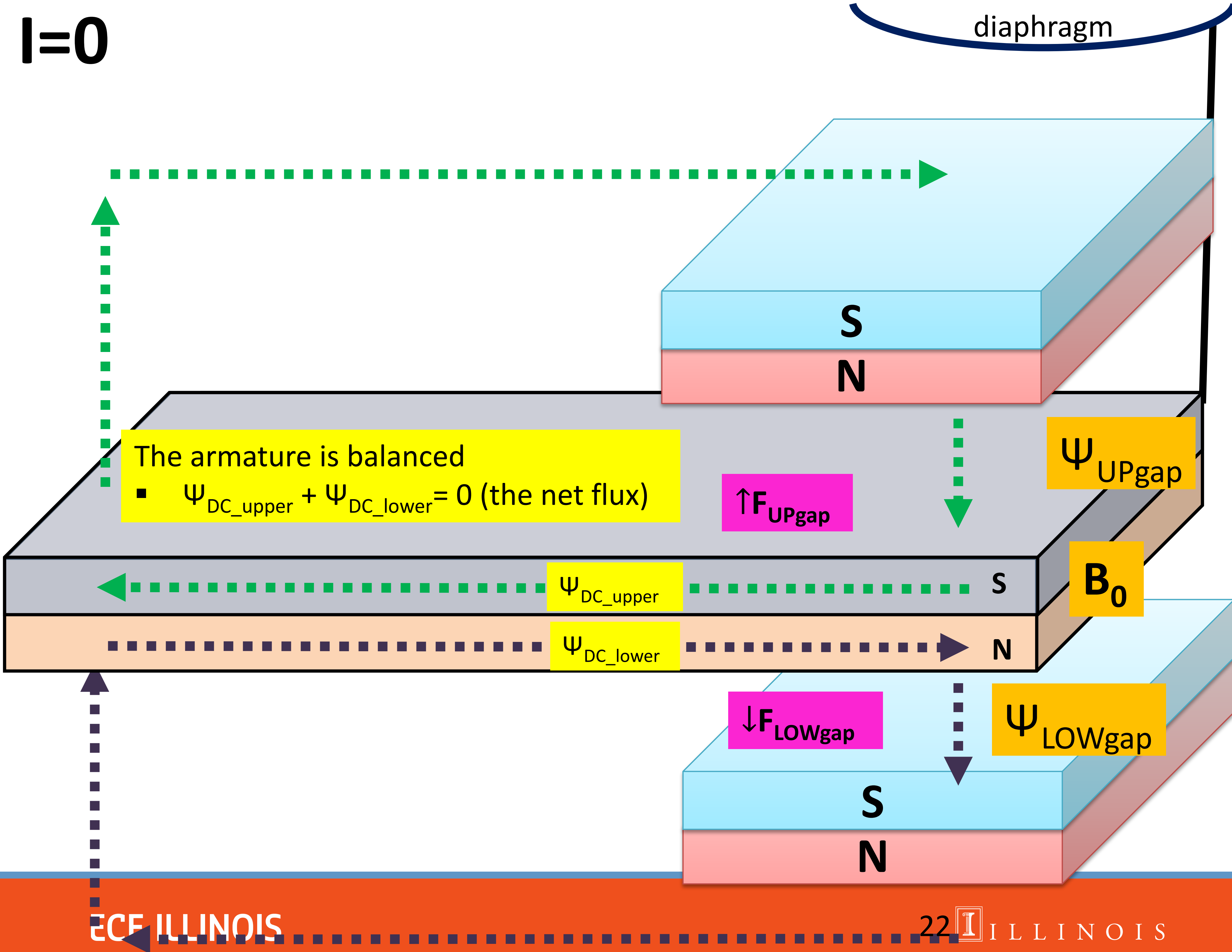
diaphragm
S
N
The armature is balanced
▪ $\Psi_{DC\_upper} + \Psi_{DC\_lower} = 0$ (the net flux)
↑F_{UPgap}
Ψ_{UPgap}
Ψ_{DC_upper}
S
B_0
Ψ_{DC_lower}
N
↓F_{LOWgap}
Ψ_{LOWgap}
S
N

I>0

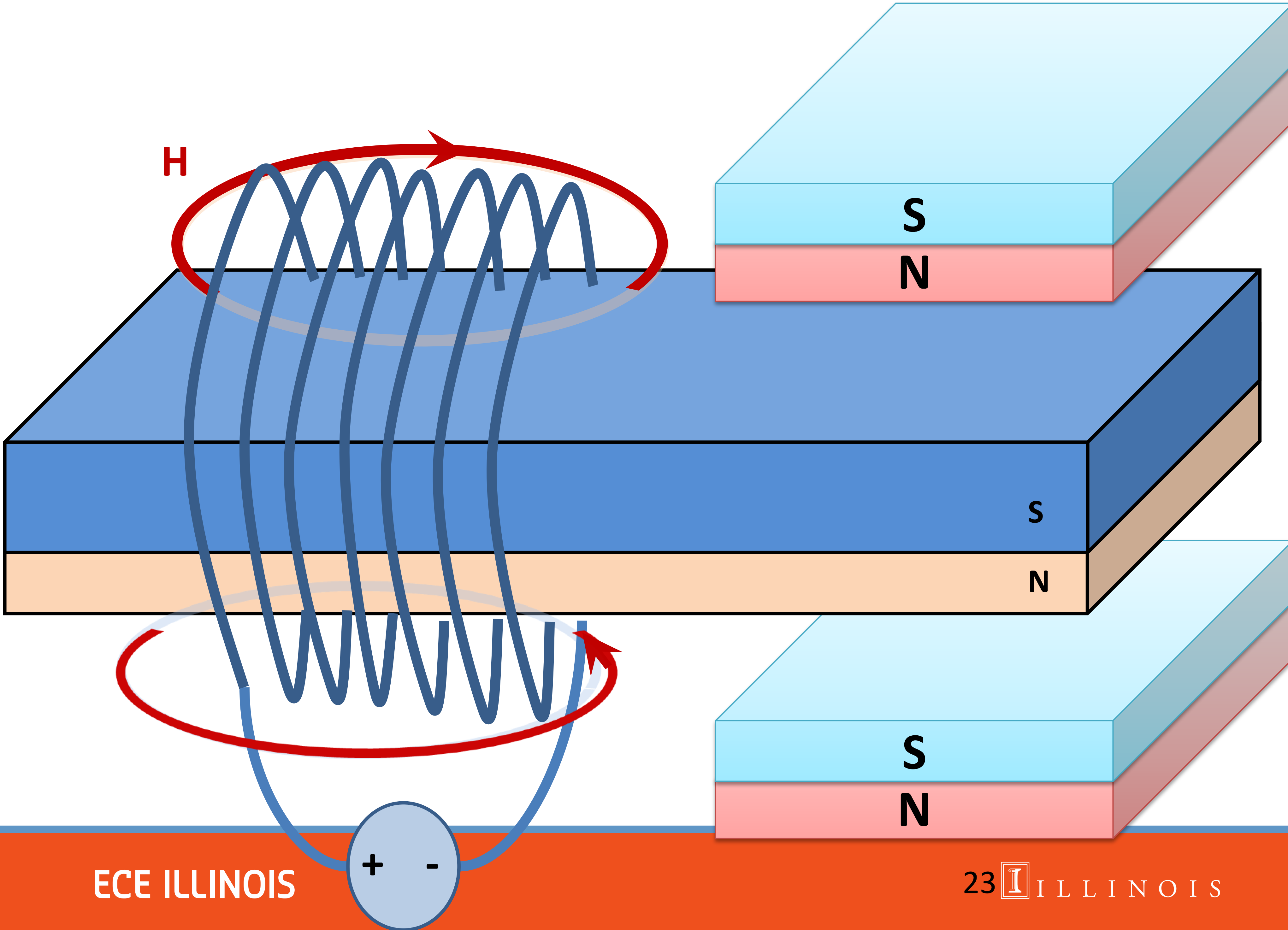

I>0

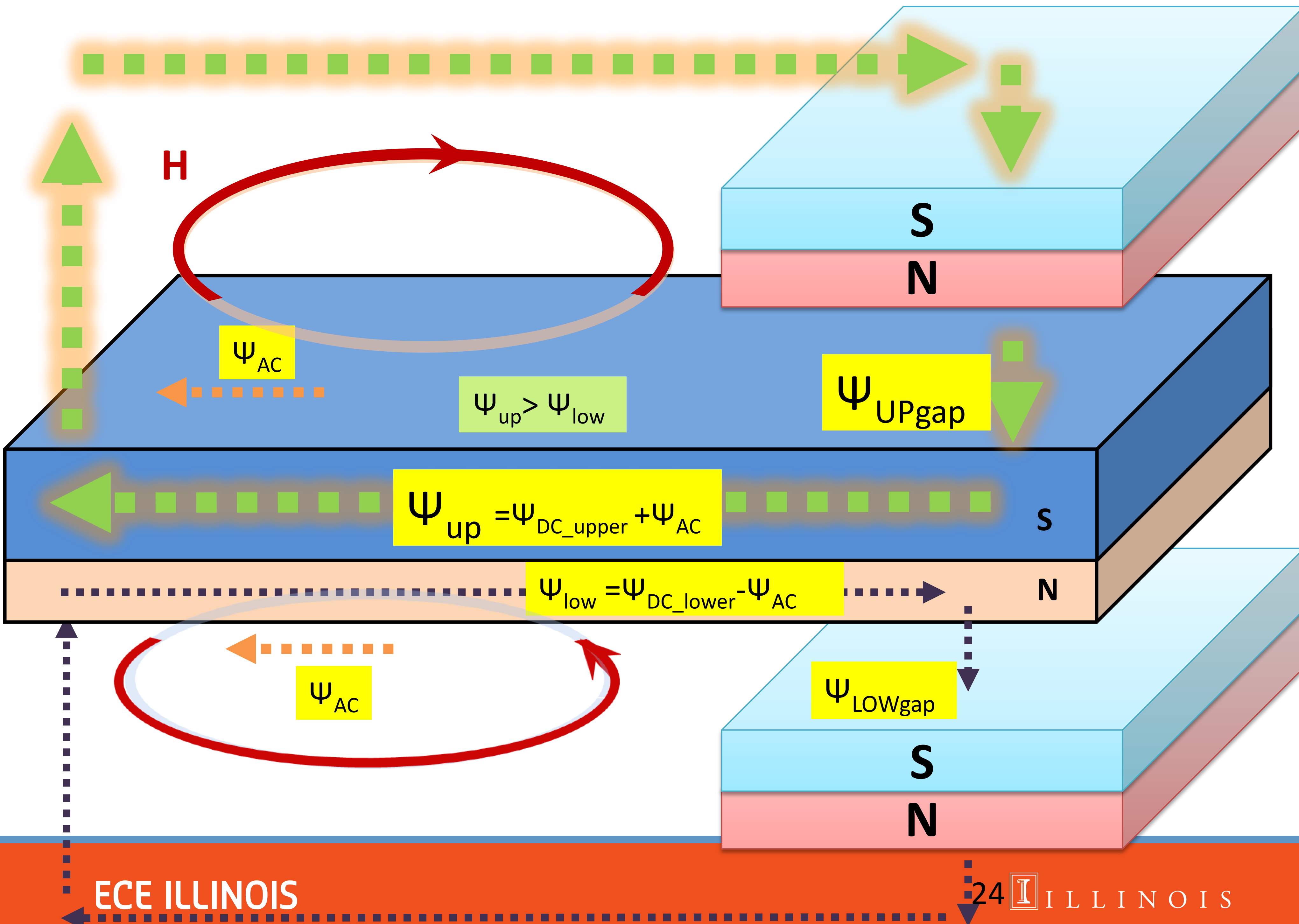
H
S
N
ΨAC
Ψup> Ψlow
ΨUPgap
Ψup =ΨDC_upper +ΨAC
s
Ψlow =ΨDC_lower-ΨAC
N
ΨLOWgap
ΨAC
S
N

I>0

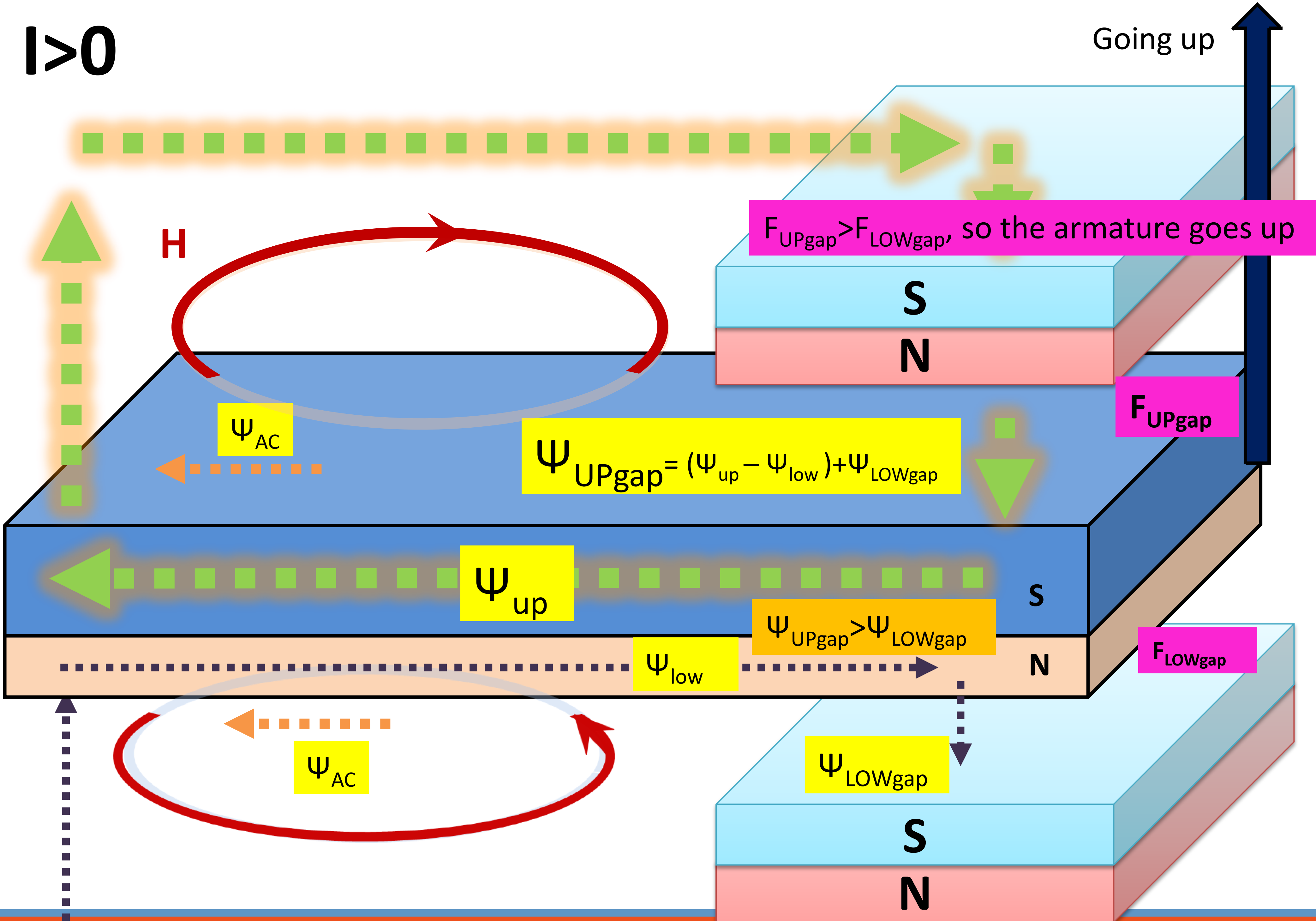

Going up
H
$F_{UPgap}>F_{LOWgap}$, so the armature goes up
S
N
F_{UPgap}
Ψ_{AC}
$\Psi_{UPgap} = (\Psi_{up} - \Psi_{low}) + \Psi_{LOWgap}$
Ψ_{up}
S
$\Psi_{UPgap} > \Psi_{LOWgap}$
Ψ_{low}
N
F_{LOWgap}
Ψ_{AC}
Ψ_{LOWgap}
S
N

- A gyrator swaps the generalized flow and force (Impedance matrix)

$$\begin{bmatrix} \Phi(\omega) \\ F(\omega) \end{bmatrix} = \begin{bmatrix} 0 & -B_0 l \\ B_0 l & 0 \end{bmatrix} \begin{bmatrix} I(\omega) \\ U(\omega) \end{bmatrix} \Rightarrow$$

Eq.1

$$\boxed{\Phi(\omega) = -B_0 l U(\omega)}$$

and

Eq.2

$$\boxed{F(\omega) = B_0 l I(\omega)}$$

Two Eqs. for an Ideal gyrator

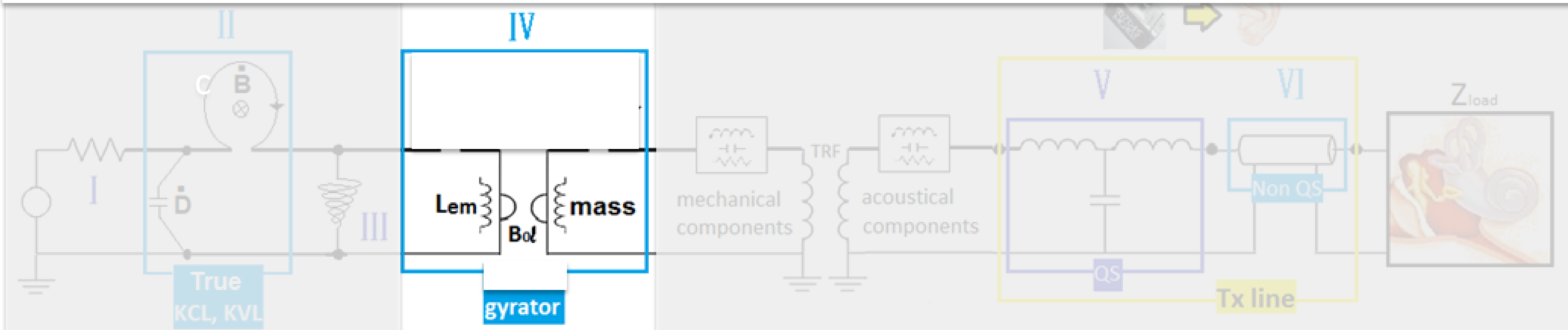

I>0

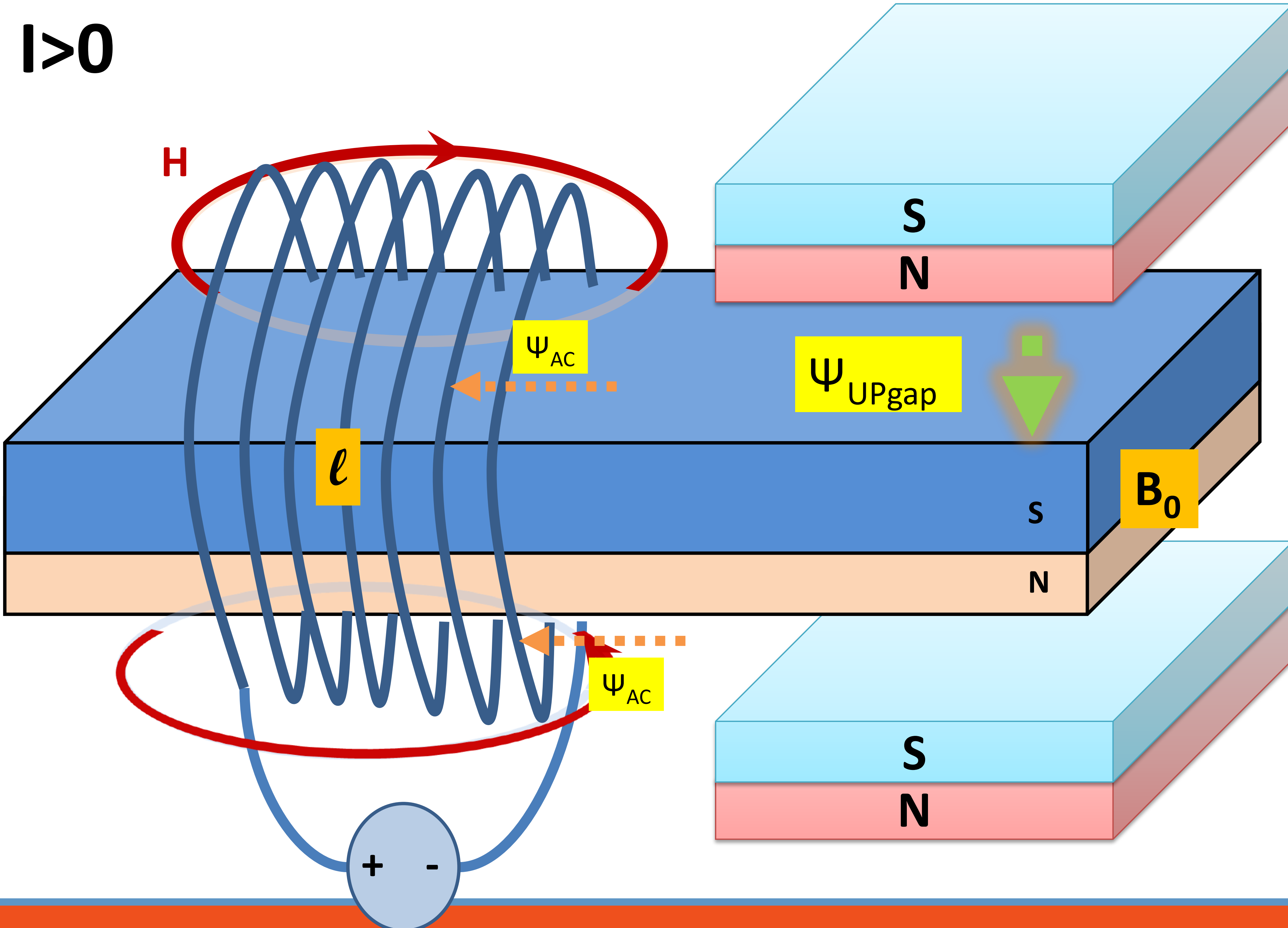

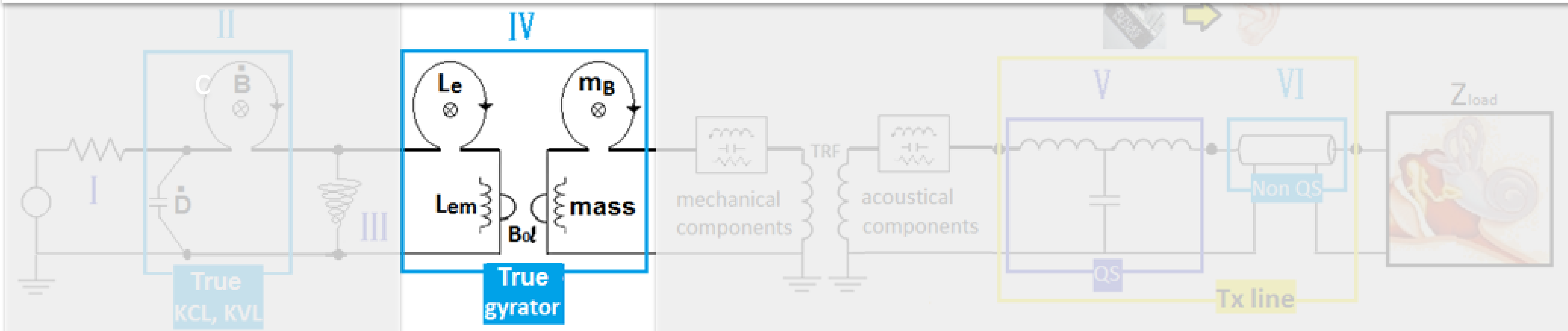

This is the basis of my suggestion, we need a non-ideal (or true) gyrator formula to include the induced (AC) magnetic fields in the system

Eddy current (solution for H)

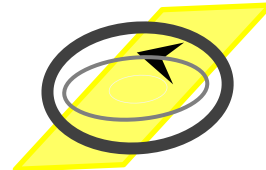

(Vanderkooy 1989)

$$\nabla \times \boldsymbol{H_z} = \boldsymbol{J_{c\phi}} + \dot{\boldsymbol{D}} \approx \boldsymbol{J_{c\phi}} = \boldsymbol{\sigma E_\phi} \text{ (1. Ampere's law)}$$

$$\nabla \times \boldsymbol{E_\phi} = -\dot{\boldsymbol{B}}_{\boldsymbol{z}} \text{ (2. Faraday's law)}$$

$$\nabla \times (\nabla \times \boldsymbol{H}) = \nabla \underbrace{(\nabla \cdot \boldsymbol{H})}_{0} - \nabla^2 \boldsymbol{H} \text{ (3. Vector identity)}$$

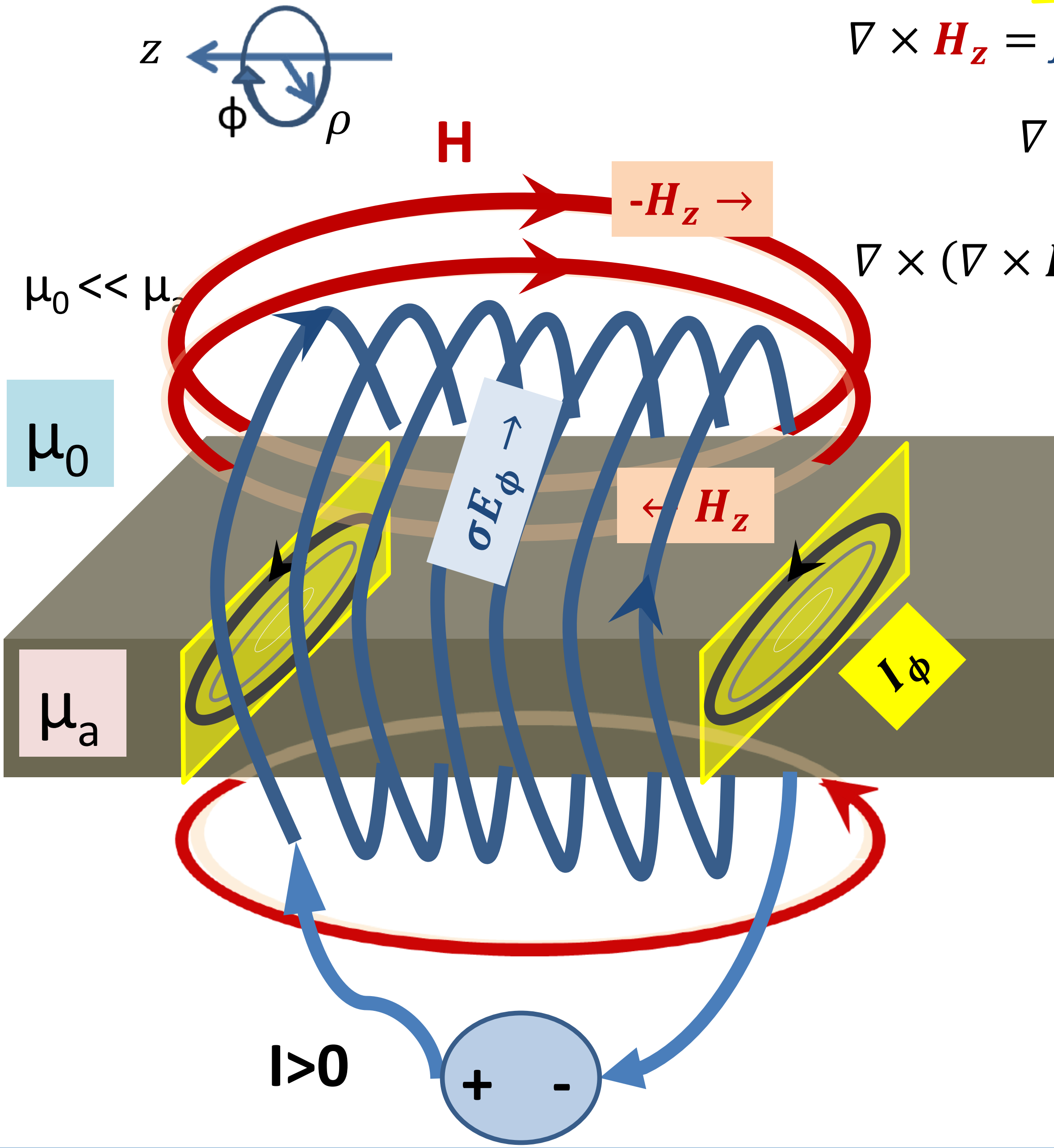

$$\nabla \times (\nabla \times \boldsymbol{H_z}) = -\nabla^2 \boldsymbol{H_z} (\because 3)$$

$$\nabla \times \left(\boldsymbol{\sigma E_\phi}\right) = -\nabla^2 \boldsymbol{H_z} \ (\because 1)$$

$$\boldsymbol{\sigma} \nabla \times \boldsymbol{E_\phi} = -\boldsymbol{\sigma} \dot{\boldsymbol{B}}_{\boldsymbol{z}} \ (\because 2)$$

Finally, $\nabla^2 \boldsymbol{H_z} = \boldsymbol{\sigma \mu_a} \frac{\boldsymbol{dH_z}}{\boldsymbol{dt}}$

In the frequency domain

$$(jk_\rho)^2 = \boldsymbol{\sigma \mu_a} j\omega$$

$$k_\rho = \pm\sqrt{\boldsymbol{\sigma \mu_a} \omega}\, e^{-\angle 45^\circ} \text{(diffusion)}$$

$$\boldsymbol{2H_z}(\rho, t) = \boldsymbol{2H_0 e^{j\omega t - k_\rho \rho}}$$

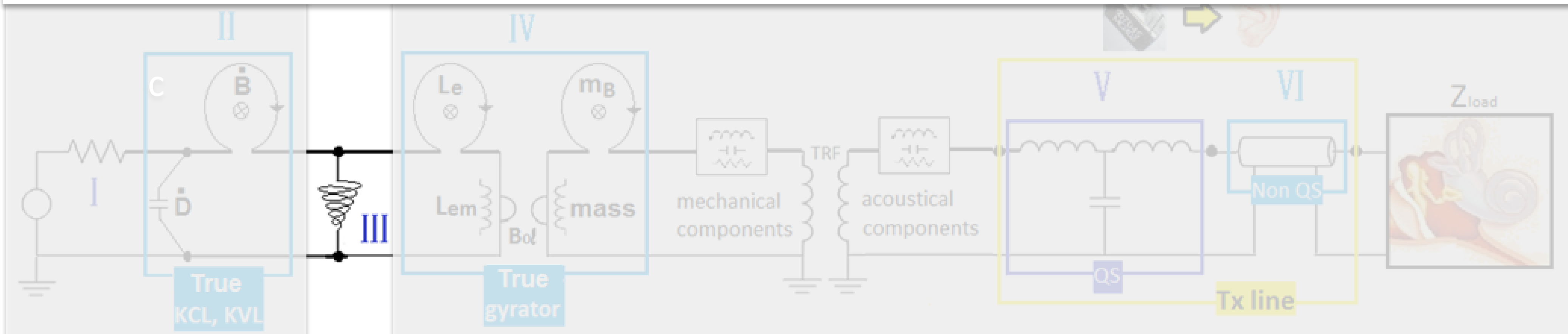

$$Z_{semi}=K\sqrt{s}$$

Application of Kirchhoff's circuit law

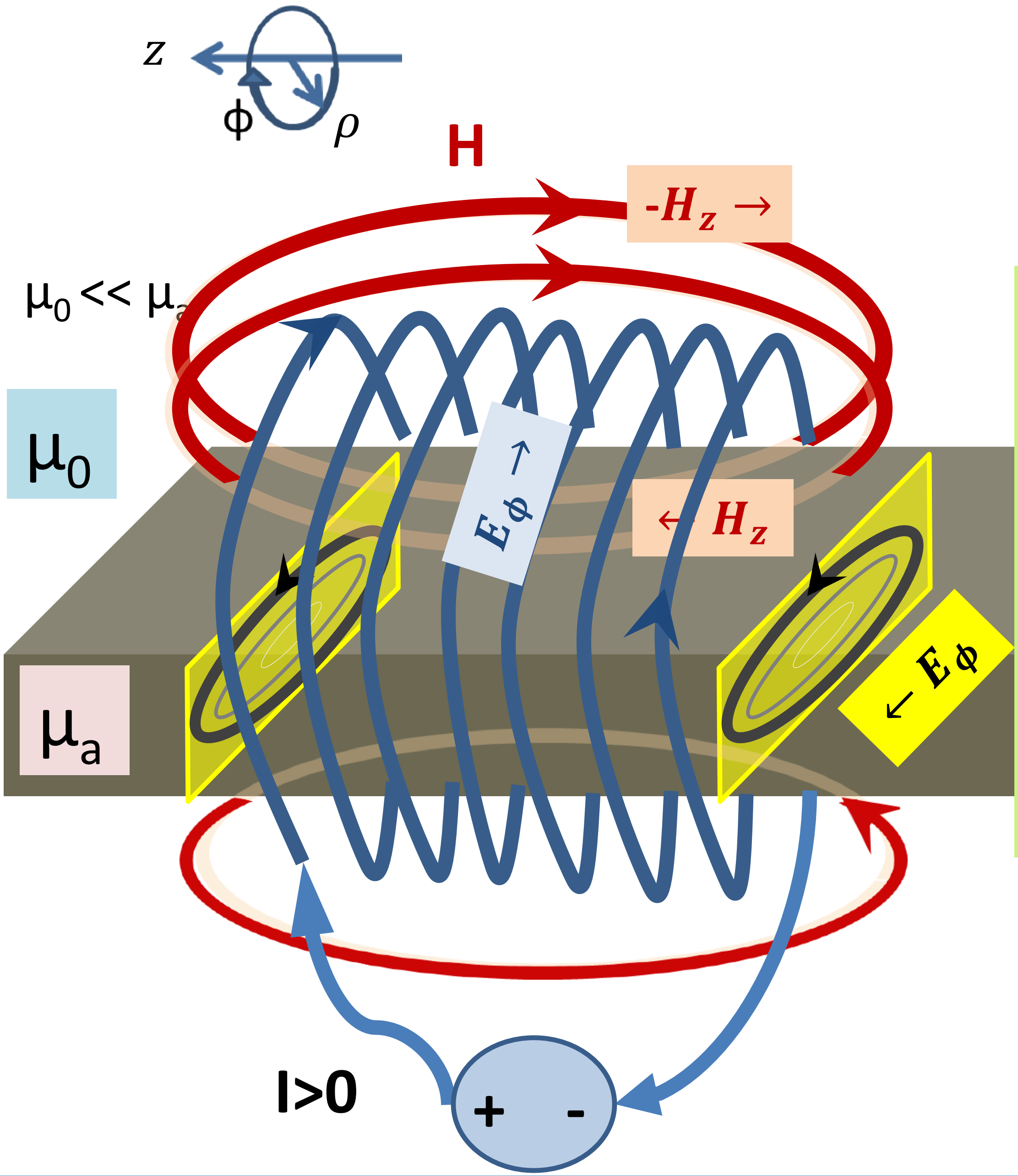

Manipulating the Faraday's law,

$$emf = \int E_\phi \cdot dl = \int \nabla \times E_\phi \cdot dA$$

$$= -\int \dot{B}_z \cdot dA = -\dot{\Psi}_a \neq 0$$

where, dA is the cross sectional area of the armature core.

- Emf is Thevenin voltage (true KVL)

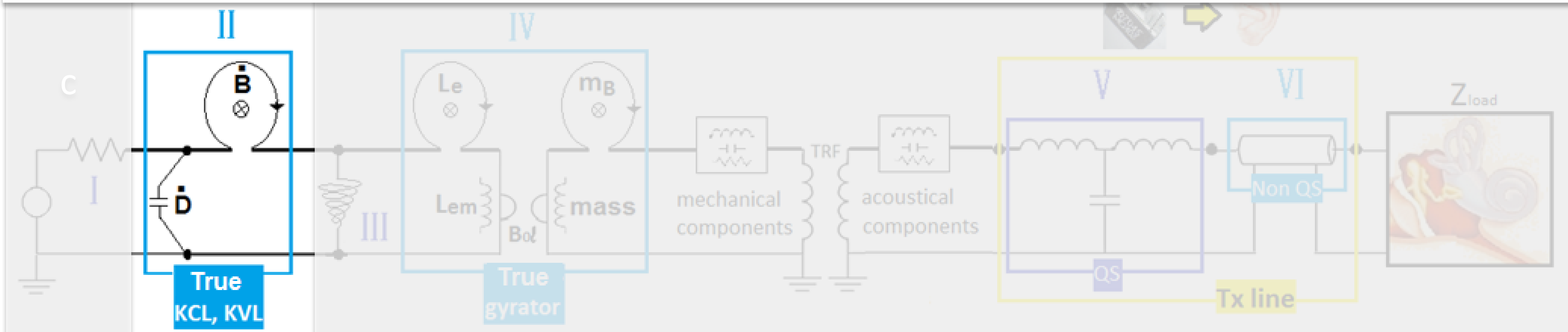

C
II
IV
V
VI
Ḃ
Le
mB
Zload
I
Ḋ
III
Lem
Bol
mass
mechanical components
TRF
acoustical components
Non QS
QS
True KCL, KVL
True gyrator
Tx line

Force on the armature and hysteresis

- Force on the armature (F_m) exists for two opposing poles across an air gap
  - Opposite poles attract and like poles repel

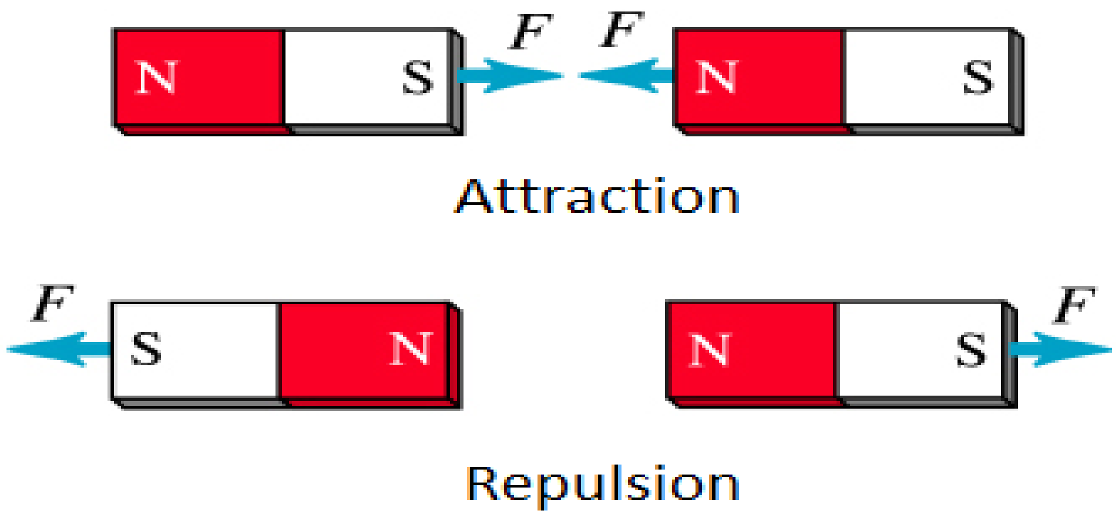

- Hysteresis can be explained by describing the F_m,

- Assumption: Core is initially not magnetized
  1. Electrical energy: $W = \int v(t)i(t)dt$ [J =N·m]
  2. $W_d = \int \frac{HlAdB}{lA} = \int \boldsymbol{HdB} = \frac{1}{\mu}\int BdB = \frac{B^2}{2\mu}$ [$\frac{J}{m^3} = \frac{N}{m^2}$]

     Faraday: $NA\frac{dB}{dt}$ Ampere: Hl/N
  3. Therefore $F_m = W_d A$

$$F_m = \frac{AB^2}{2\mu} = \frac{A_g {B_g}^2}{2\mu_0} = \frac{{\Psi_g}^2}{2\mu_0 A_g} [N]$$

$$W_d = \int \frac{HlAdB}{lA} = \int \boldsymbol{HdB} = \frac{1}{\mu}\int BdB = \frac{B^2}{2\mu}\ [\frac{J}{m^3} = \frac{N}{m^2}]$$

The green formula can be related to the famous hysteresis loop graph

- x-axis and y-axis represent H and B
- Hysteresis loss: subtraction of two regions
- A typical hysteresis phenomenon of Ferro-magnetic material

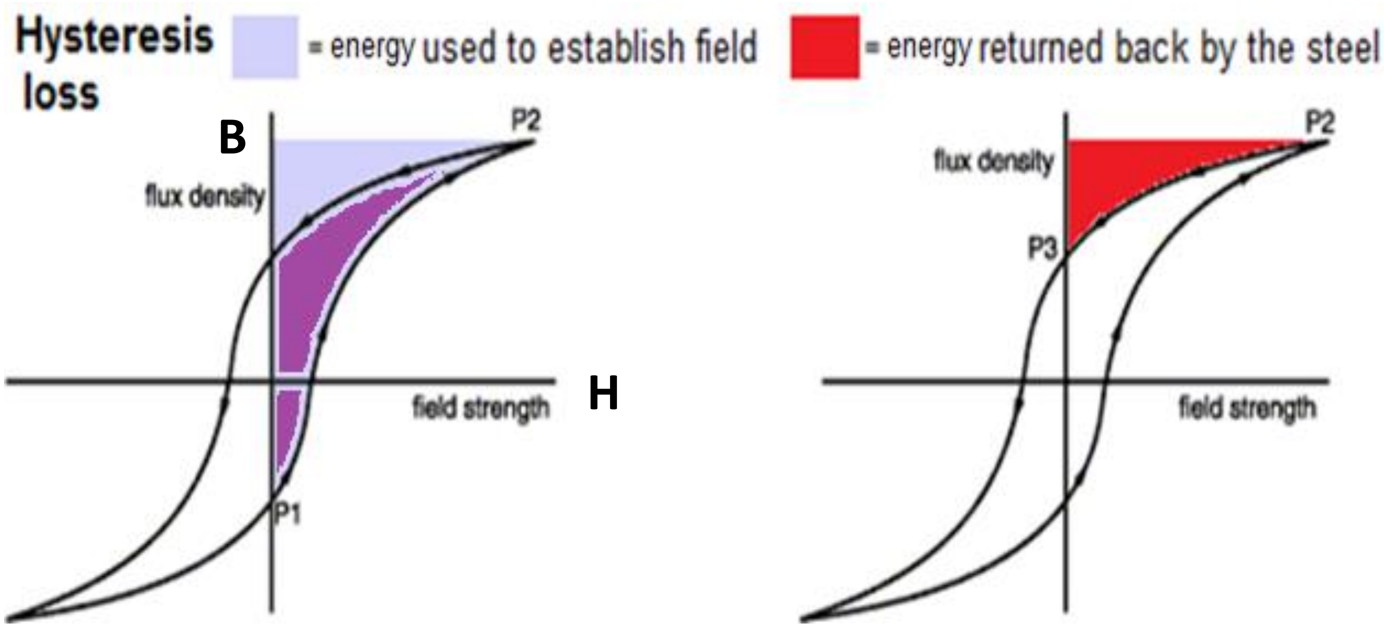

(http://info.ee.surrey.ac.uk/Workshop/advice/coils/power_loss.html#eddy)

I am interested in BAR's operational region

- Hunt 1954, Ch. 7, Moving armature transducer systems
- BAR type receivers are operating in a lens shaped region
  - The region can be linearly approximated
  - Centered at Ψ_0 (due to the permanent magnet)
  - Alternating Ψ_i
  - $F_m = \frac{{\Psi_g}^2}{2\mu_0 A_g} = \frac{(\Psi_0+\Psi_i)^2}{2\mu_0 A_g}$
    $= \frac{{\Psi_0}^2+2\Psi_0\Psi_i+\boxed{{\Psi_i}^2}}{2\mu_0 A_g}$ → Non-linear part Second harmonic distortion
  - If Ψ_i=$\Psi_I \cos\omega t$, then ${\Psi_i}^2 = \frac{1}{2}{\Psi_I}^2(1+\cos 2\,\omega t)$

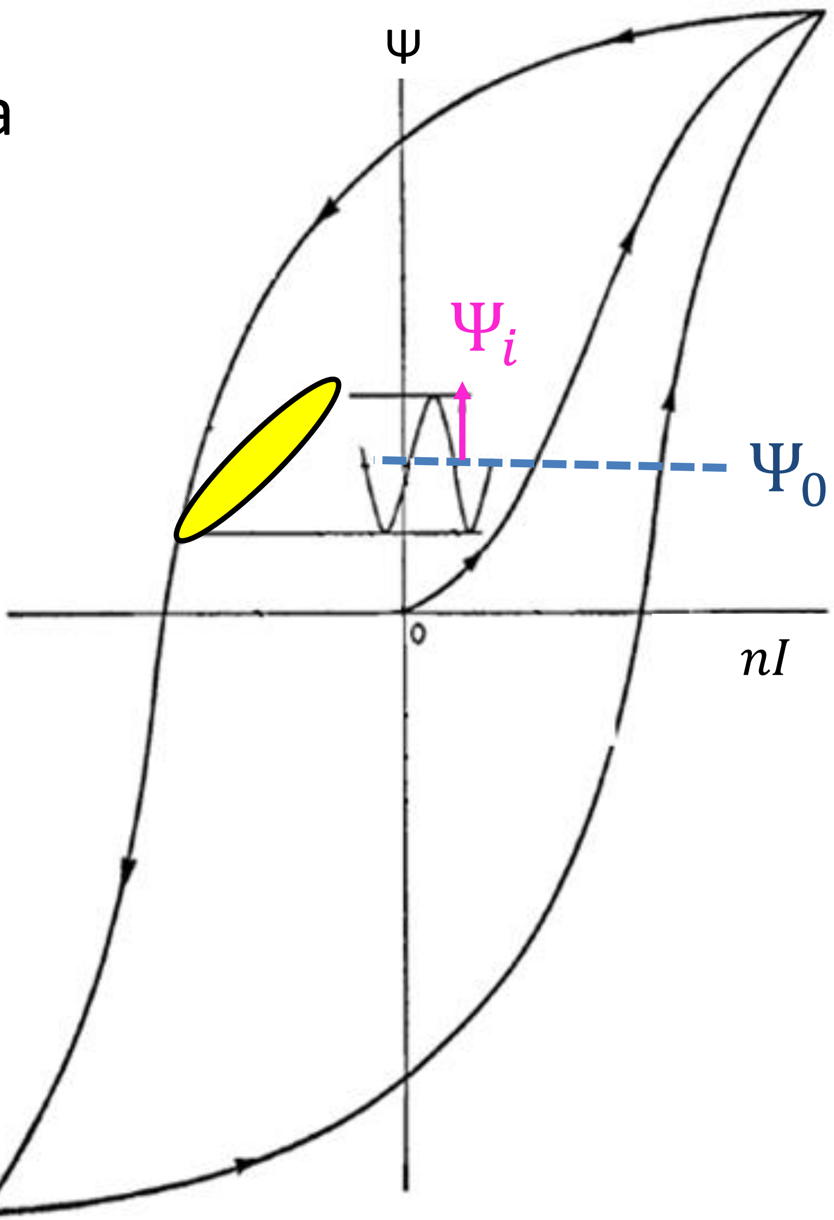

Non linear behavior observation in electrical input impedance (Z_{in})

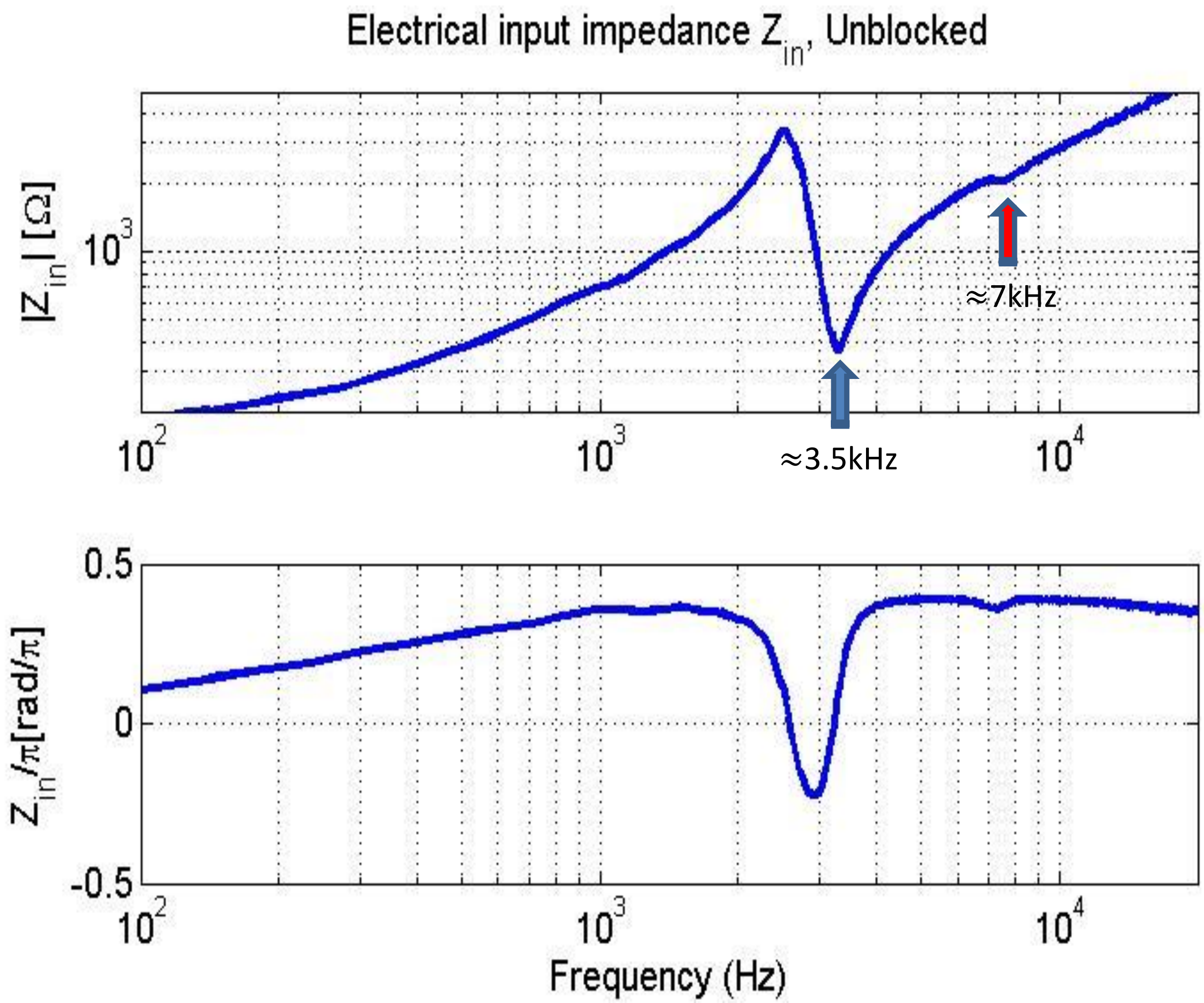

The Hunt parameters

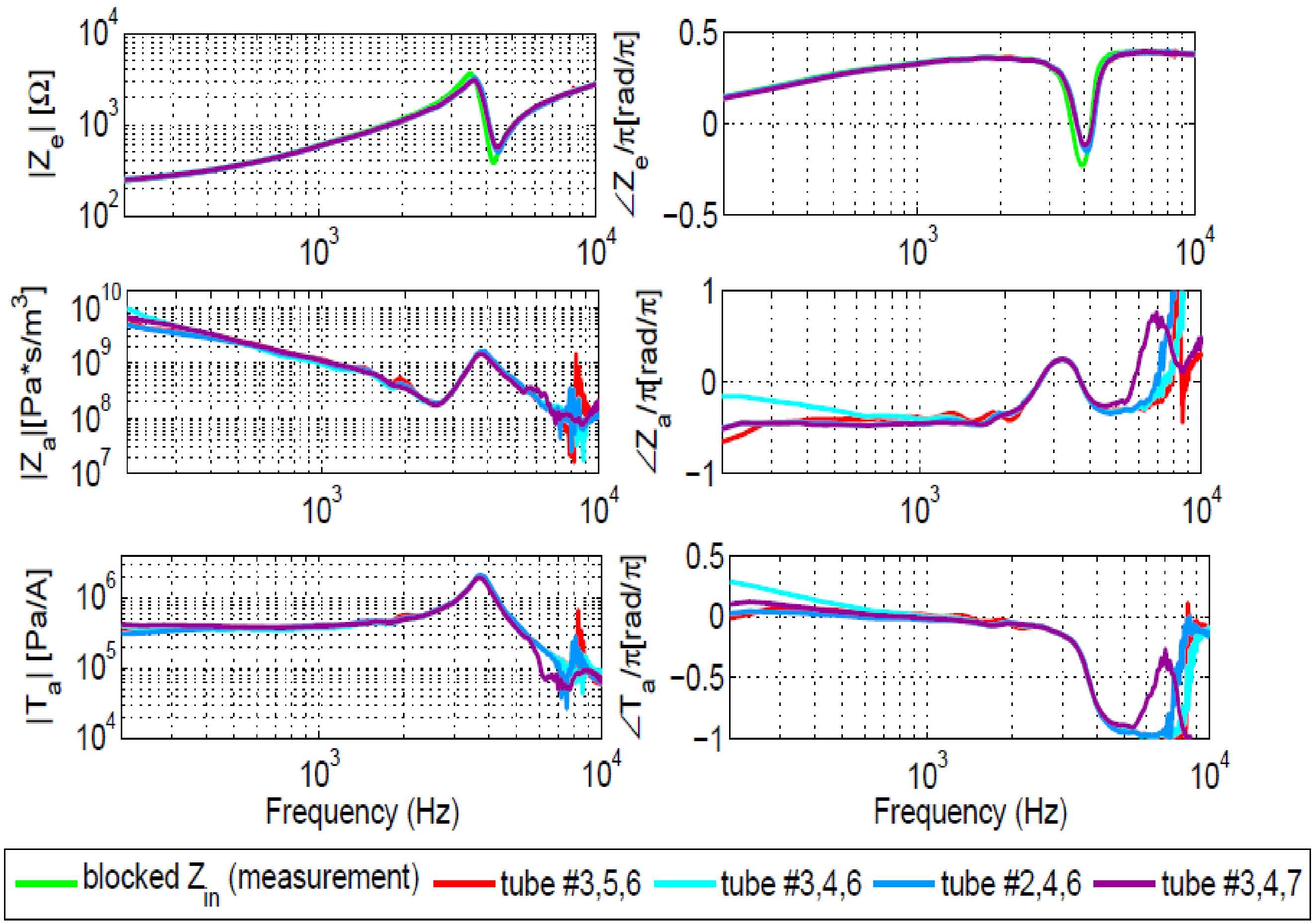

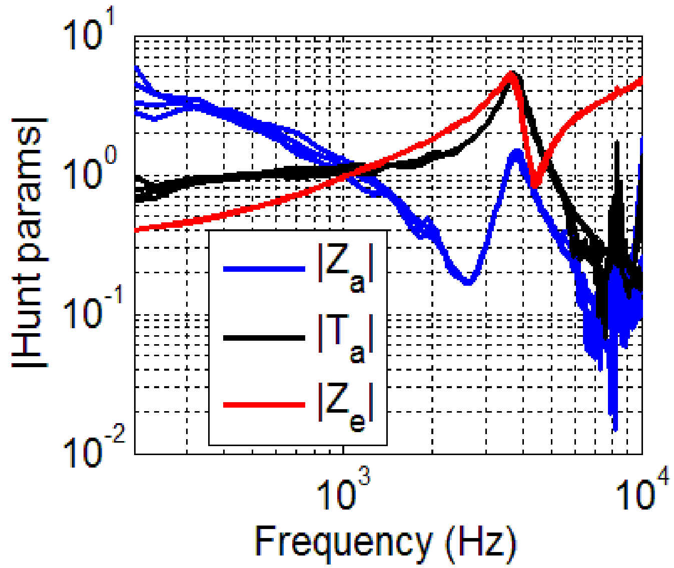

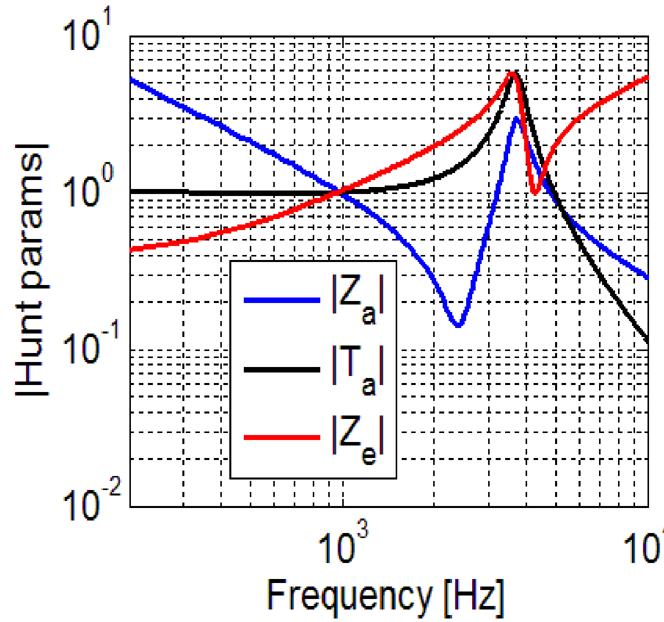

Quasi-static (QS) and delay

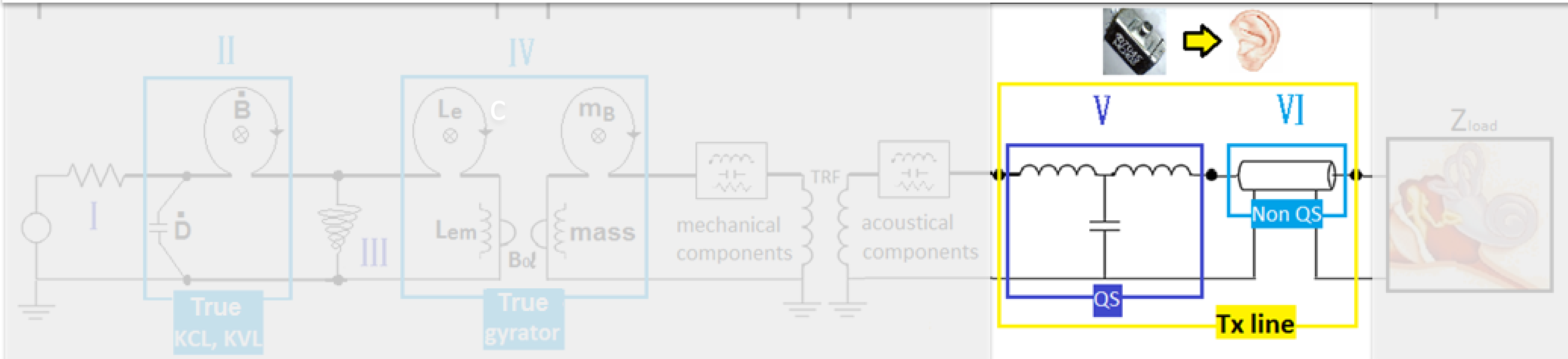

- QS in the frequency domain: the wavelength is much larger than the dimension of the system in question (ka<<1)
  - ✓ In the time domain: delay (τ) << a/c
- When we deal with a physical system, such as ear canal, transmission line representation is simpler and more intuitive way to model the delay accurately
  - ✓ Lumped element can mimic the system almost identically, but the number of elements increases with bandwidth
  - ✓ Tx-line: No worry about the band limitation of the system

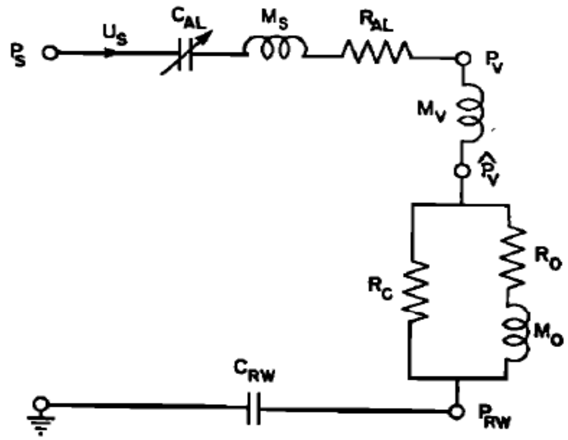

(a) Original electrical network representation of the impedance of the stapes and cochlea by Lynch et al (1982)

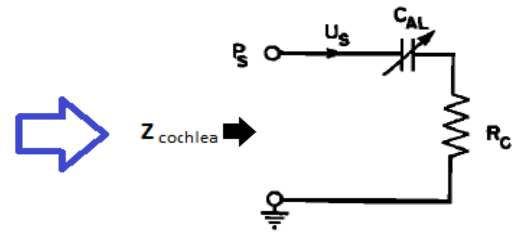

(b) Simplified version of (a) with minimum lumped circuit elements without delay line

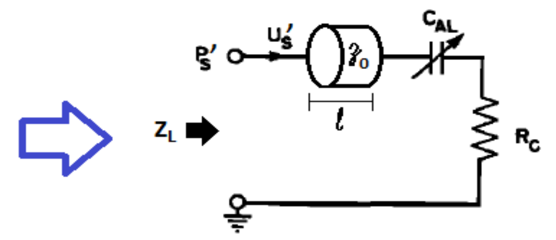

(c) Delay (transmission line) is added to (b)

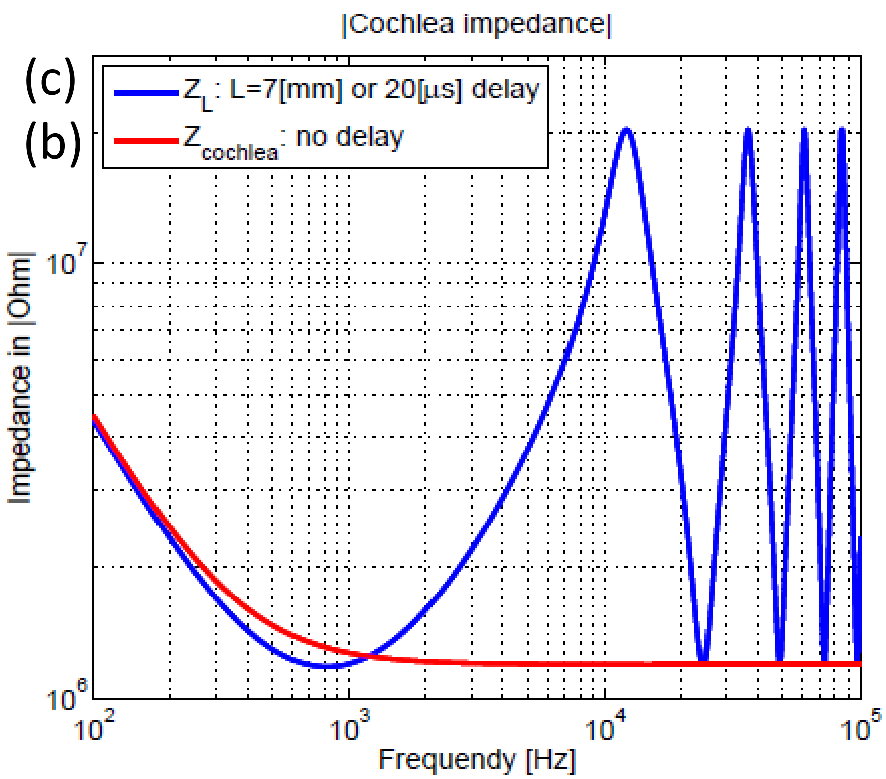

- Blue line (c): $Z = \frac{1+\Gamma}{1-\Gamma}$, where $\Gamma = e^{-sl/c}$.
  - ✓ $\tau = \frac{l}{c}$: a pure delay, s: Laplace frequency
  - ✓ $\Gamma = \pm 1$: impedance poles and zeros
- Red line (b): simplified QS version (no delay)
  - ✓ We may use lumped elements to represent the delay, but circuit complexity increases
- Transmission line is the proper tool to describe a pure delay

Conclusion I from theory part

- Principles of the BAR's operation include the Eddy-current effect, hysteresis loss, and force on the two magnets

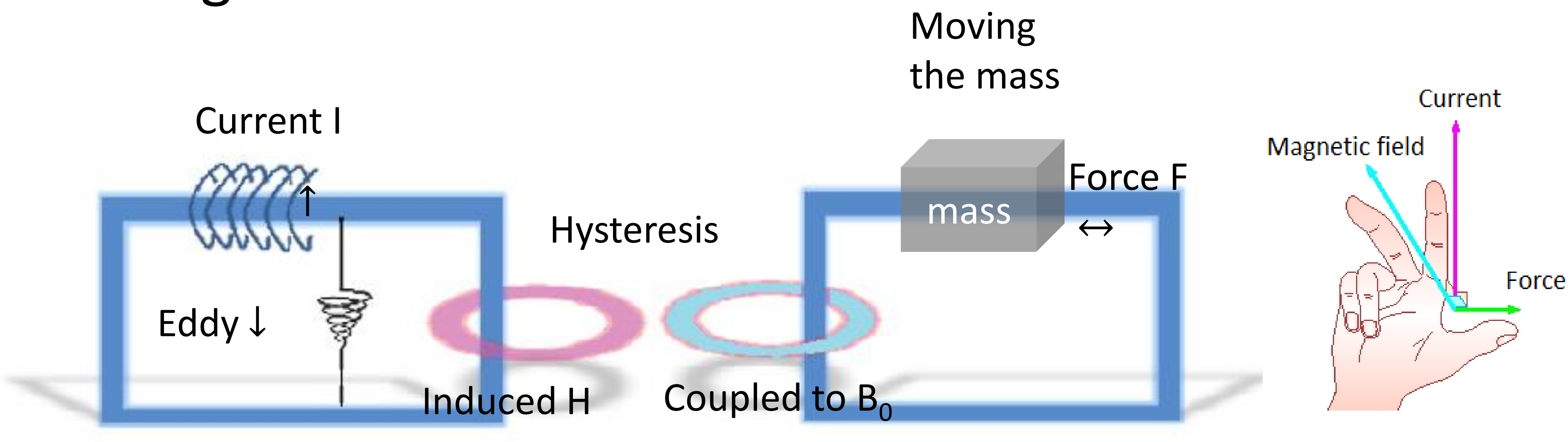

- This work will provide a fundamental, clearer insight into this type of BAR system

II. Experimental part

- Experiments to support (verify) my theory
  - Electrical input impedance measurements
  - Laser vacuum measurements
  - Pressure measurements
- Hearing measurement probe manufacturing
  - Existing probe study
  - Manufacturing and evaluation

Electrical input impedance measurements

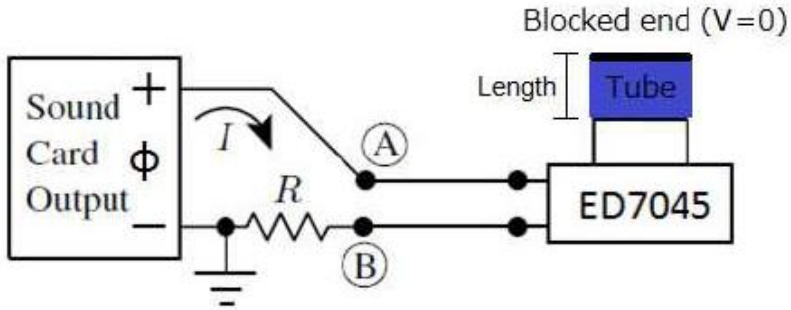

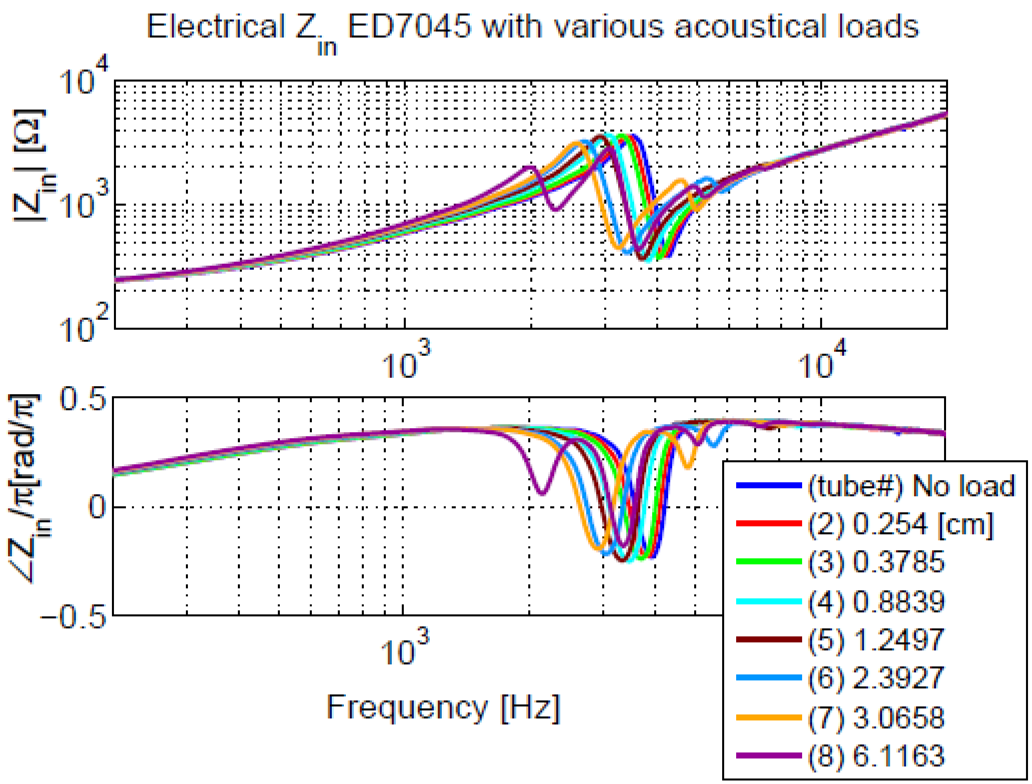

$$Z_{in} = \frac{\Phi_A - \Phi_B}{I} = \frac{\Phi_A - \Phi_B}{\Phi_B/R} = R\left(\frac{\Phi_A}{\Phi_B} - 1\right).$$

- **Used for the Hunt parameter calculation**

Laser vacuum measurements

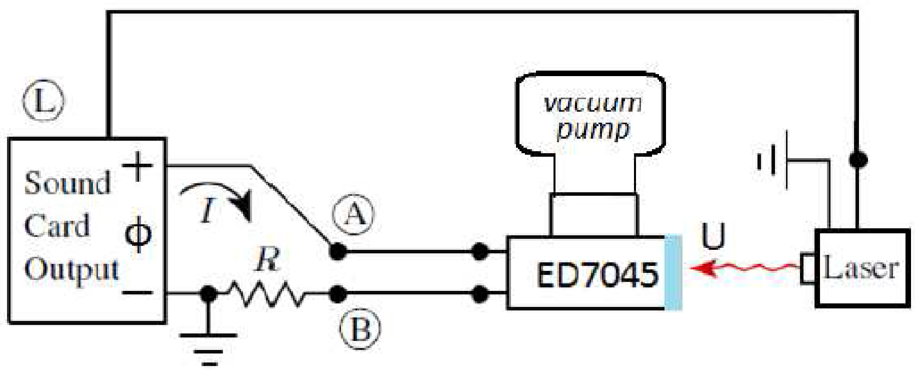

Pressure measurements

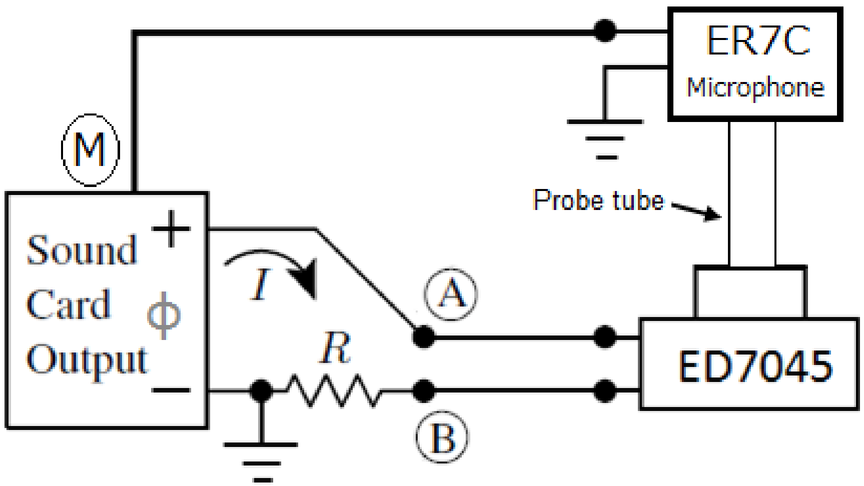

- A portion of the transducer's case was carefully removed
- Then a thin plastic window was glued on, to reseal the case

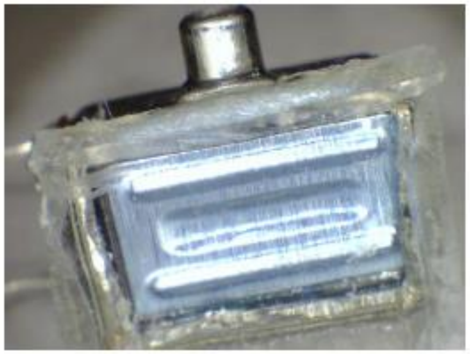

- The circled 'M' means an input from the ER7C microphone

II. Experimental part

- Experiments to support (verify) my theory
  - Electrical input impedance measurements
  - Laser vacuum measurements
  - Pressure measurements
- Hearing measurement probe manufacturing
  - Existing probe study
  - Manufacturing and evaluation

Existing probe study: ER10C (Etymotic Research)

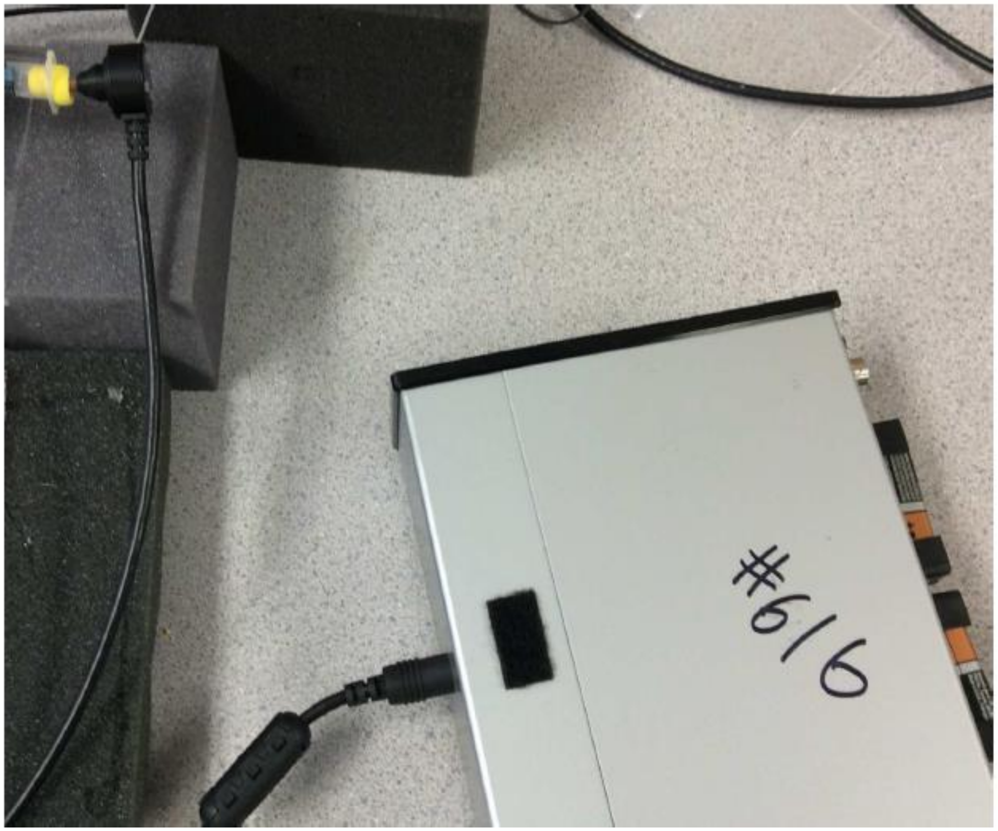

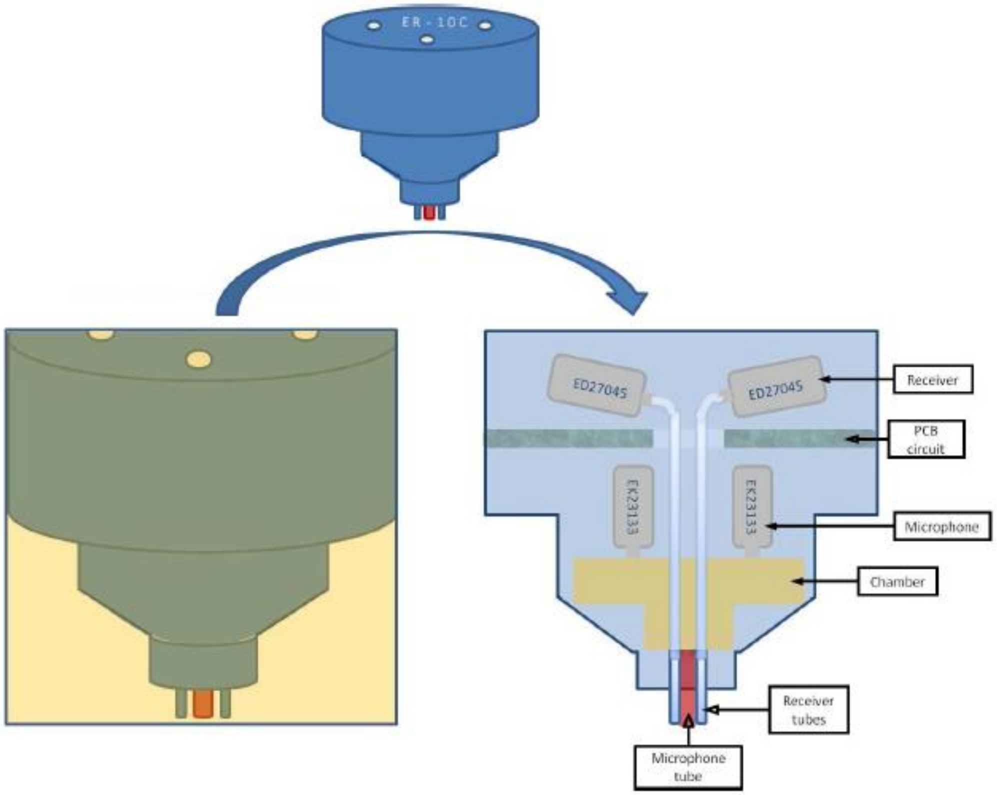

- Otoacoustic emission (OAE, sounds given off by the inner ear when the cochlea is stimulated by a sound) measurement device
- Two speakers and microphones are separated internally across the PCB circuit, microphones are placed ahead of the receivers

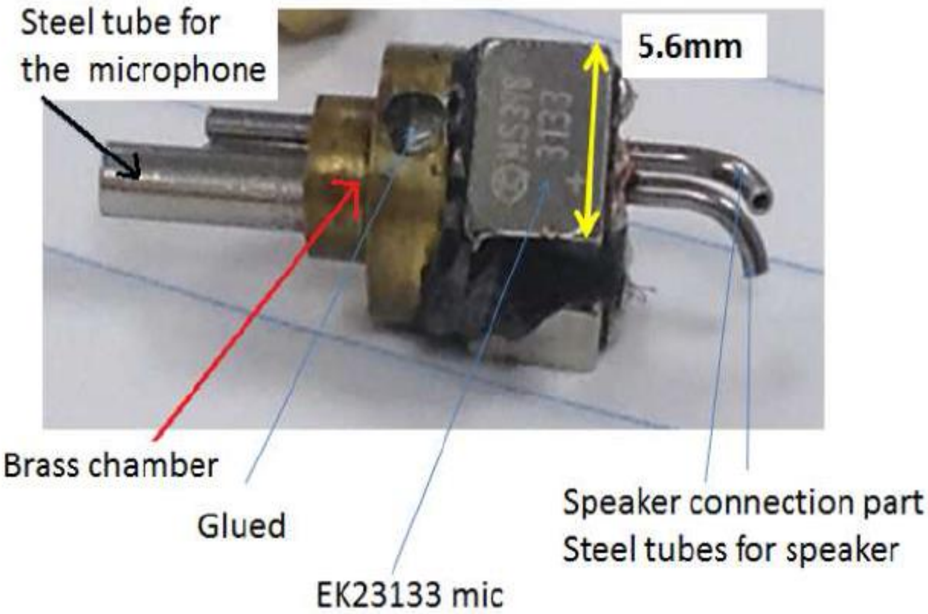

(a)ER10C microphone holder

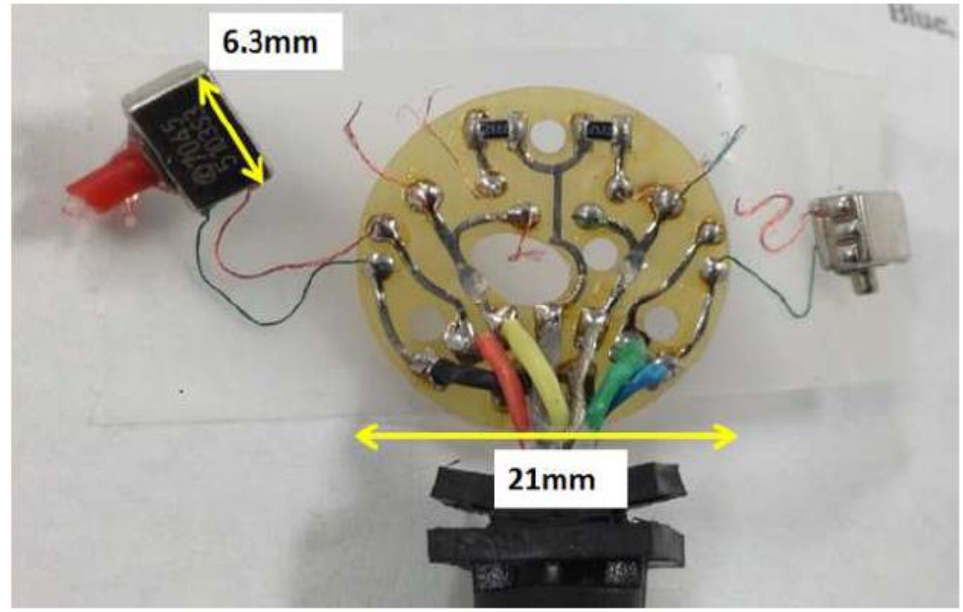

(b)ER10C circuit board part

- The microphones are firmly attached to the chamber
- The speakers are attached to steel tubes via a soft rubber tubes, floated in the air
  - The air is a best damper, vibrational crosstalk from the speakers can be reduced

Issues with ER10C

- The small number of competitors in the market, users have not had many alternatives to the system
- The size of the probe is too big for infants
- Handling it without extreme caution may lead to malfunction of the probe (delicate device)
- The result of the measurement depends too much on the condition of the foam tip that is inserted in the subject's ear canal
- Above 6 kHz, calibration (always) fails (the most critical problem)

Problem: above 6 kHz, calibration fails

Mimosa acoustics, HearID Calibration control screen

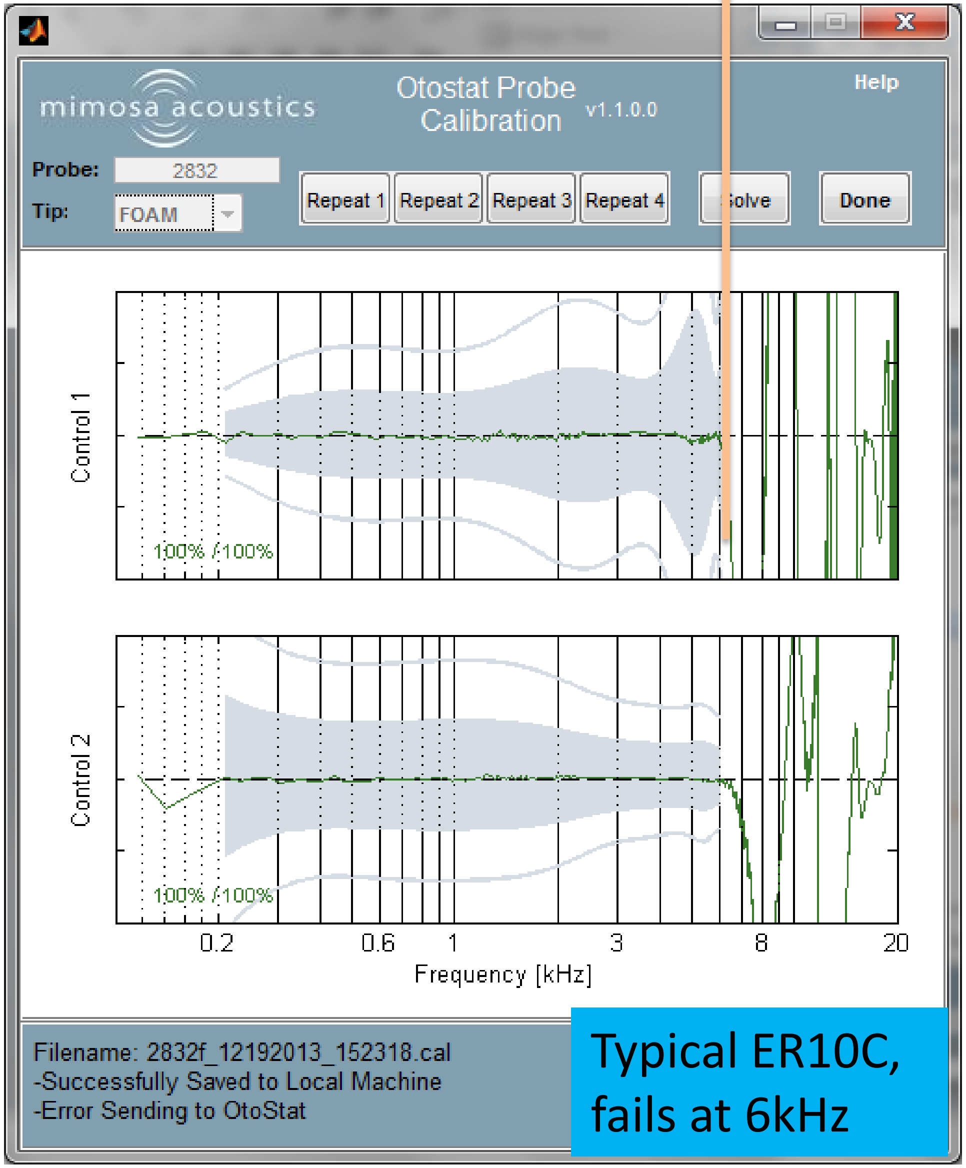

Typical ER10C, fails at 6kHz

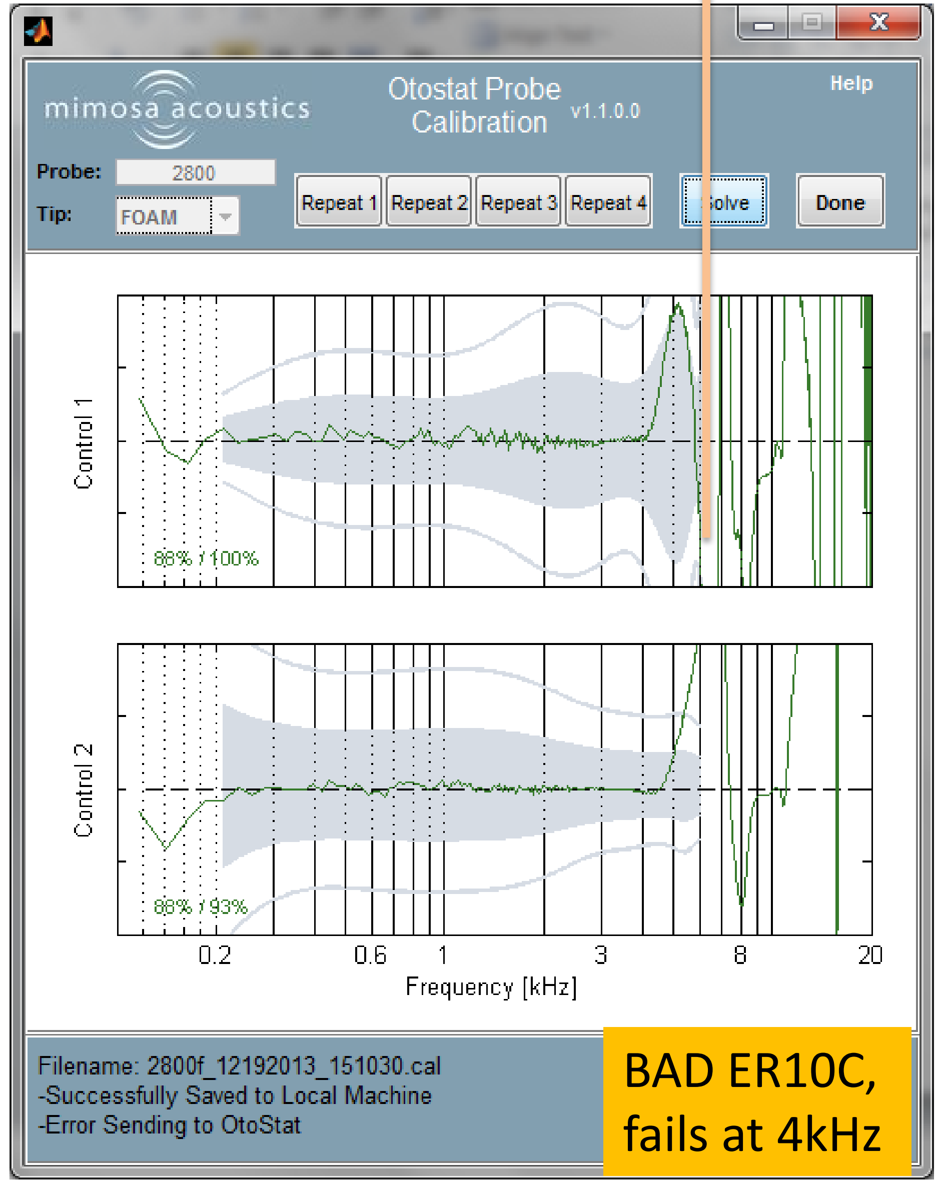

BAD ER10C, fails at 4kHz

Observation: crosstalk in the system

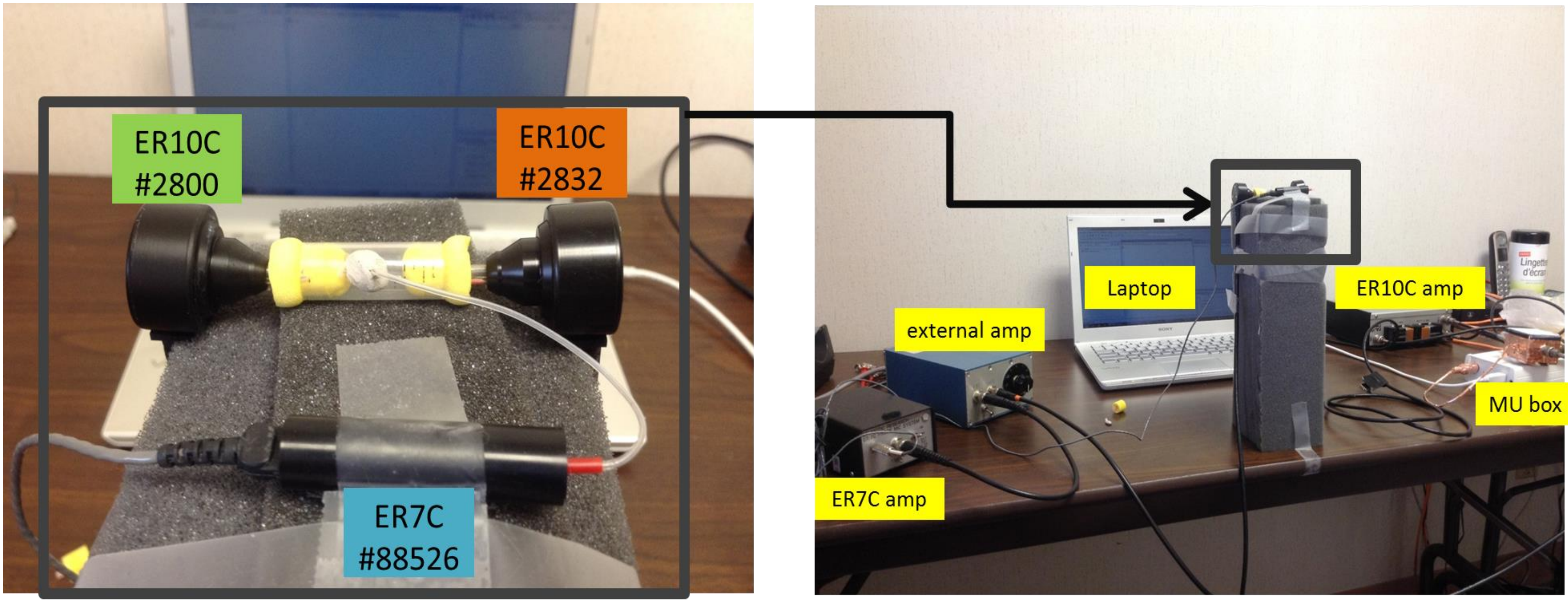

- We blocked the microphone hole on the ER10C foam tip to decouple the microphone sound path to the ER10C

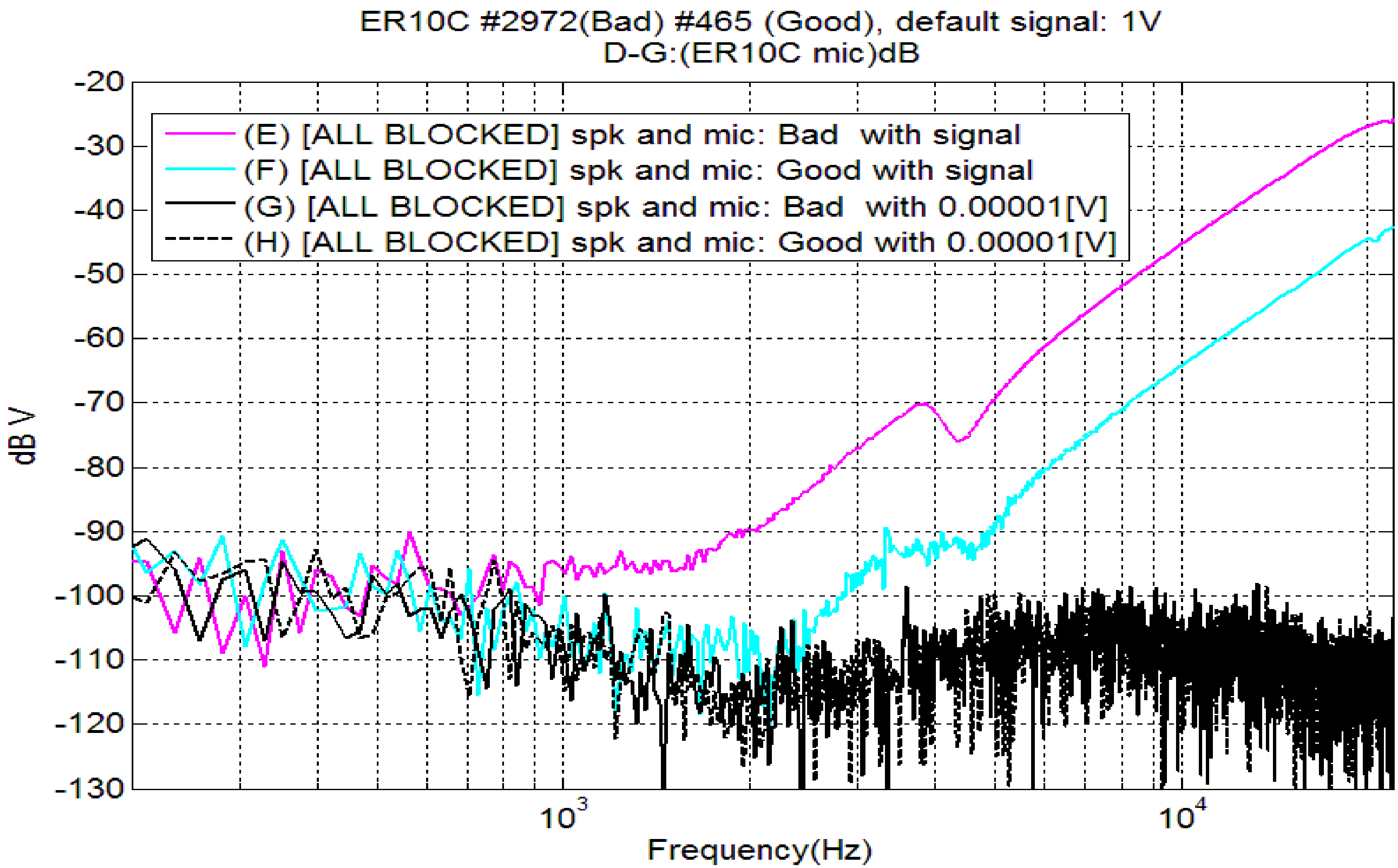
ER10C #2972(Bad) #465 (Good), default signal: 1V
D-G:(ER10C mic)dB
(E) [ALL BLOCKED] spk and mic: Bad with signal
(F) [ALL BLOCKED] spk and mic: Good with signal
(G) [ALL BLOCKED] spk and mic: Bad with 0.00001[V]
(H) [ALL BLOCKED] spk and mic: Good with 0.00001[V]
dB V
-20
-30
-40
-50
-60
-70
-80
-90
-100
-110
-120
-130
10^3
10^4
Frequency(Hz)

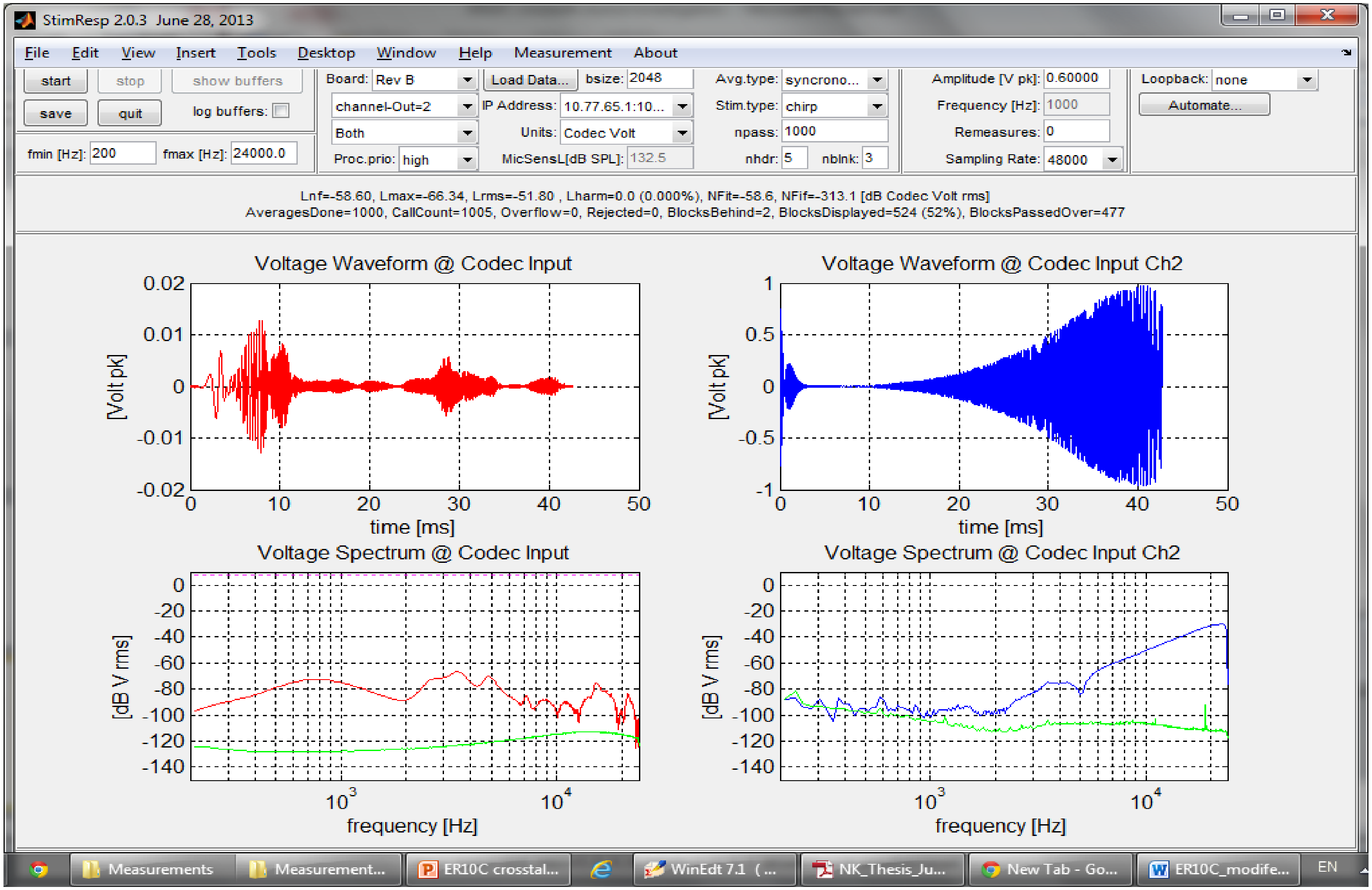

- Any signal that is shown on the right side of this figure (blue) can be assumed as the internal crosstalk (20dB/Oct)

Hypothesis, approach, and expectation

- The long wire attached to the ER10C probe contributes to the electrical crosstalk (capacitive coupling) in high frequency
- To lower the electrical crosstalk, we attached an external amplifier (close to the probe head)
- The available calibrating frequency range will be extended above 6 kHz

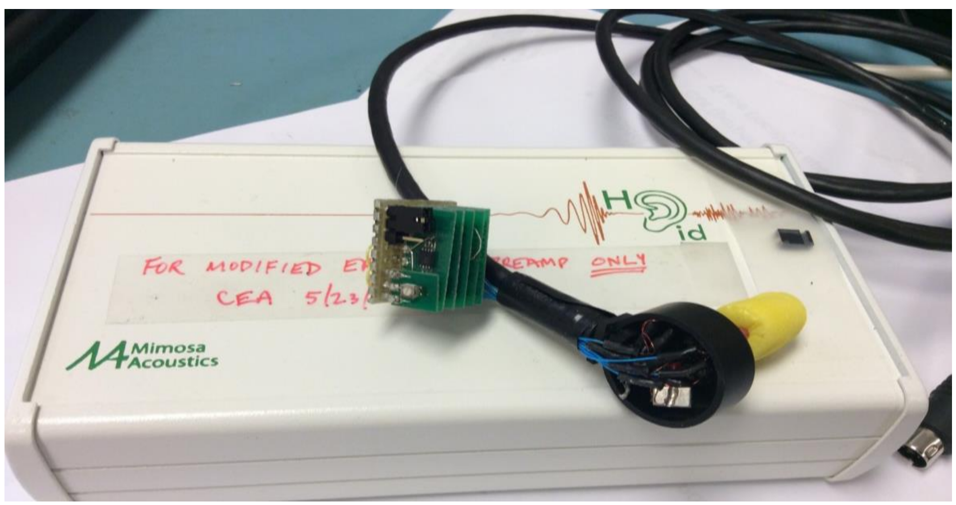

- **Results: the calibration frequency range has been extended to 11kHz**

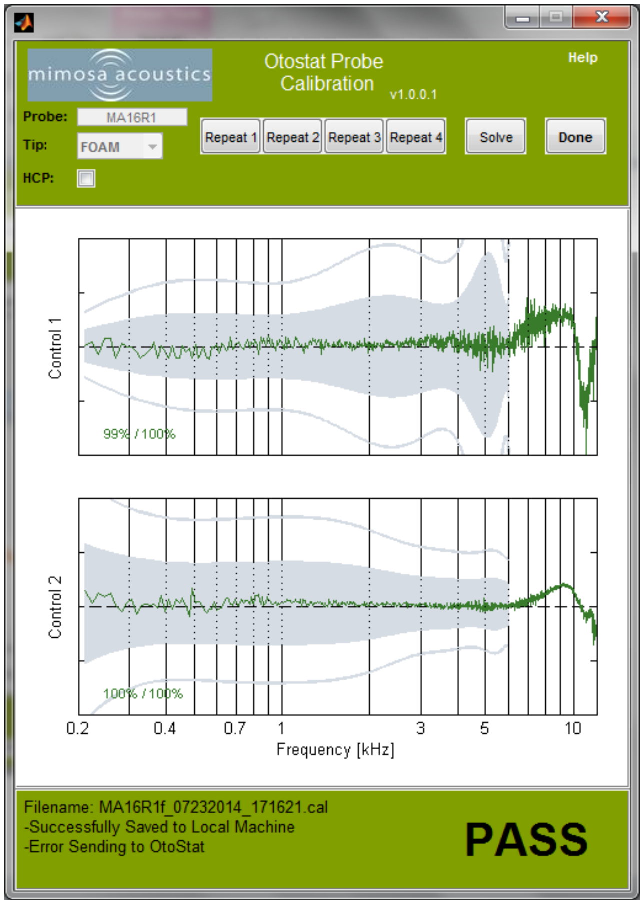

Crosstalk before/ after

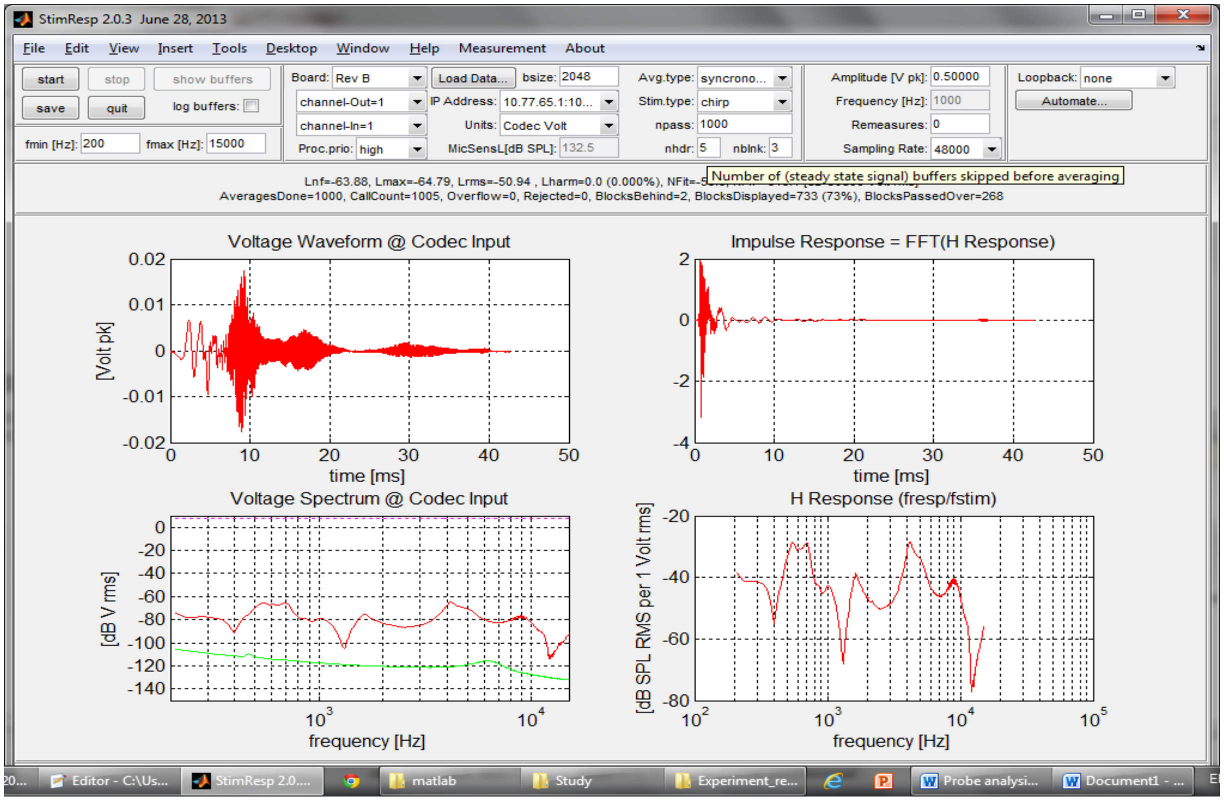

BEFORE

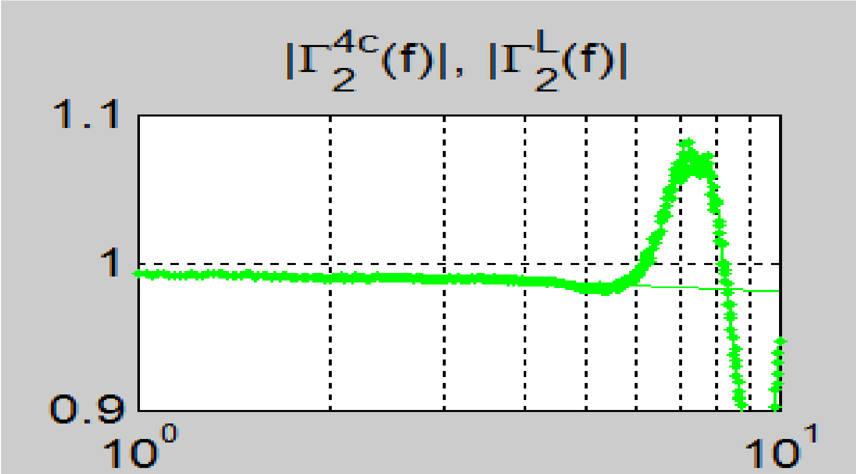

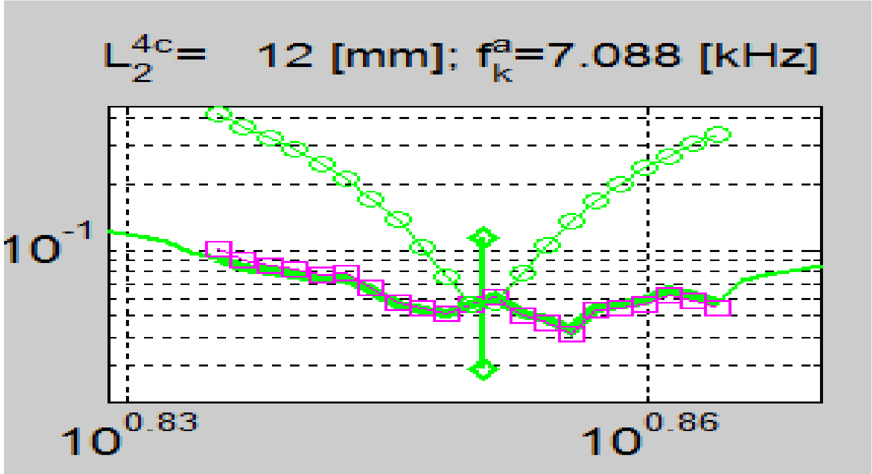

AFTER

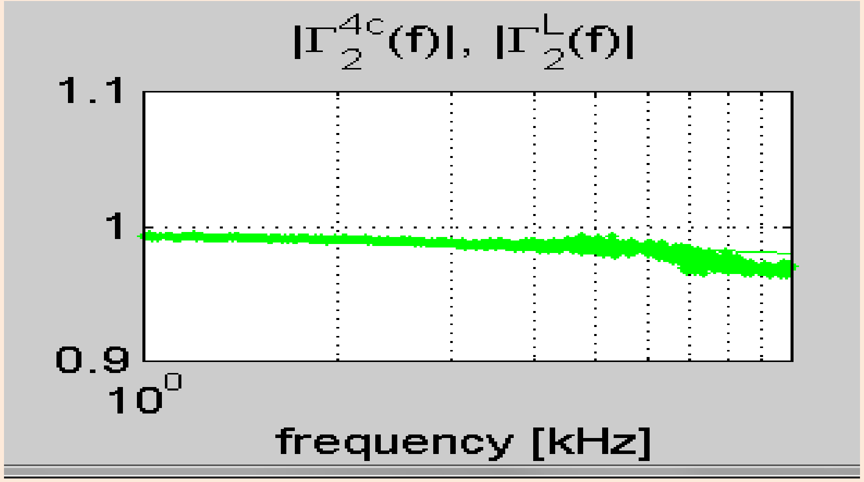

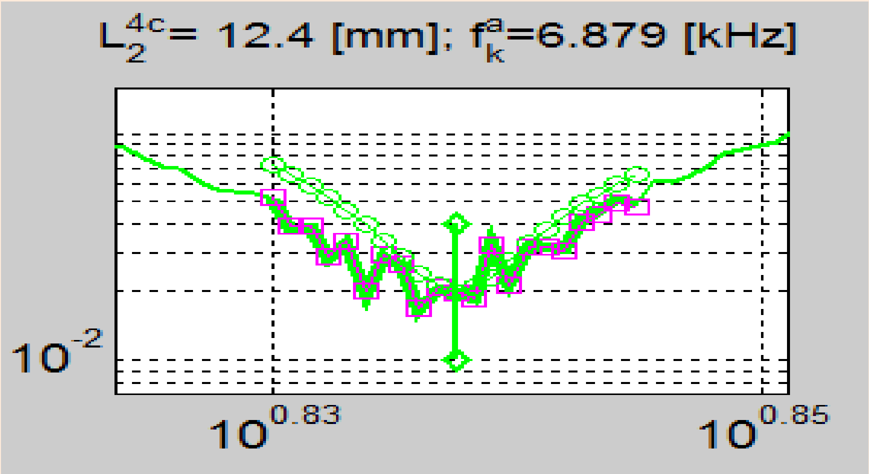

|Gamma| in each cavity

1. **Theoretical, length based:**

   $\Gamma_k^L = e^{-2L_k \kappa(f)}$ (thin line)

2. **Experimental:**

   $\Gamma_k^{4C} = (1 - Y_k^{4c})/(1 + Y_k^{4c})$ (thick line)

   where $Y_k^{4c} = U_s/P_k - Y_s$

Pressure null ($c_0/4L_k \approx 45/Lk$)

1. **Theoretical (green circle):**

   $P_k^L = P_s/(Y_s + Y_k^L)$

   where $Y_k^L = (1 - \Gamma_k^L)/(1 + \Gamma_k^L)$

2. **Experimental (pink square)**

   $P_k^{4c} = P_s/(Y_s + Y_k^{4c})$

Probe manufacturing and evaluation

- Learning from lots of trials (and errors)

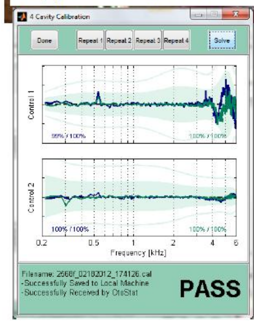

- These probes use TWFK 60173 receivers
- stable and continuous 4-cavity calibration pass

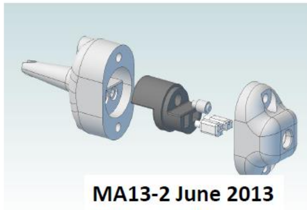

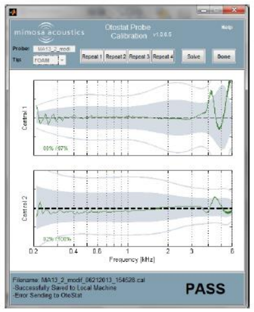

MA 12-4

- Receivers
  - GQ 30710 (37ohm at 1kHz)
  - GQ 30783 (90ohm at 1kHz)
- Microphone
  - EK23133 (ER10C microphone)
- Physical structure looking at the electrical terminal end of the probe

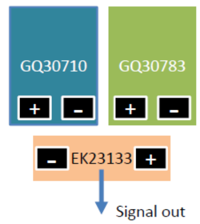

MA15-1

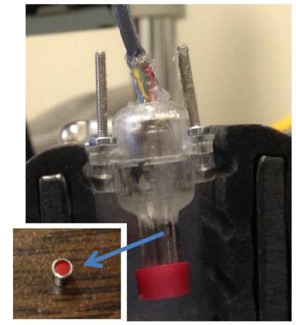

2.2k Ohm acoustic resistors (red) for receivers

- Microphone (1): FG-23652
- Receivers (2) TWFK60173
- 2.2k ohm(red) acoustic resistors (2) for receivers (Knowles BF 1921)
- Casing: 2 pieces, front and back
  - soft material compared to other MA15 series due to the manufacturing setting (not high resolution)
- Silicon glue, super glue, and liquid electrical tape

23

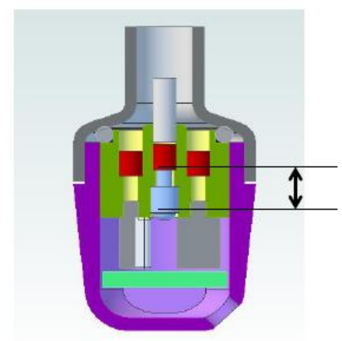

The receivers are generating sound behind the microphone

- But in MA16 current design, the position of the microphone is ahead of the receivers without considering the steel tube length.

MA12-1

- OUT: Knowles TWFK 60173 (2) receivers
- In: Knowles EM23346 (1) microphone
- ILO's coupler

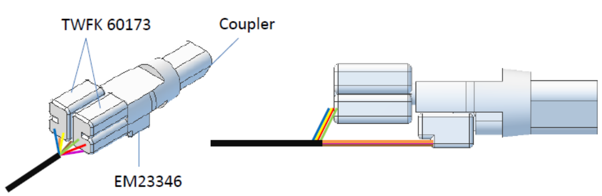

Future direction

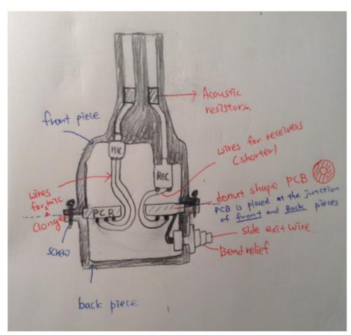

Key idea

- PCB board
- An amp is attached in probe's body (not shown in this picture)

94

Sensitivity factors (≈0.8cc cavity)

@ 996.1Hz	ER10C	MA12-3	ILO-TE	MA12-1	MA 12-2
Microphone	EK23133	EK23133	EM23346	EM23346	EM23346
Acoustic resistor	No	No	Yes	No	Yes
Foam tip	Yes	No	Yes	No	No
Cavity type	A	A	A	B	B
Microphone sensitivity [volt_peak/Pa]	0.1304	0.0301	0.1845	0.43829	0.1460
Receiver sensitivity [Pa/volt_peak]	2.1e4	1. e5	6 e3	456	7.5e4

Design Option	a: Without acoustic resistors		b: With acoustic resistors ( )	
1	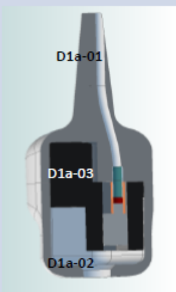	**Code: D1a** **Case (SLA, clear)** • Front part(tip): D1a-01 • Back part: D1a-02 **Middle part** • Black rubber: D1a-03	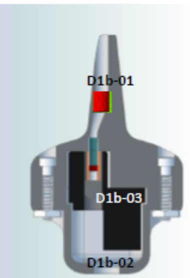	**Code: D1b** **Case (SLA, clear)** • Front part(tip): D1b-01 • Back part: D1b-02 **Middle part** • Black rubber: D1b-03
2	MA15-3 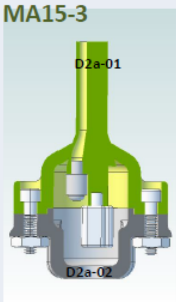	**Code: D2a** **Case (SLA, clear)** • Front part(tip): D2a-01 • Back part: D2a-02 **No middle part**	MA15-1,2,4,5 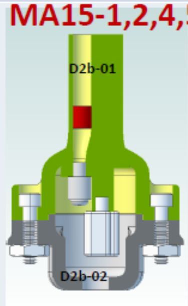	**Code: D2b** **Case (SLA, clear)** • Front part(tip): D2b-01 • Back part: D2b-02 **No middle part**

▪ MA16 & MA17 simulator

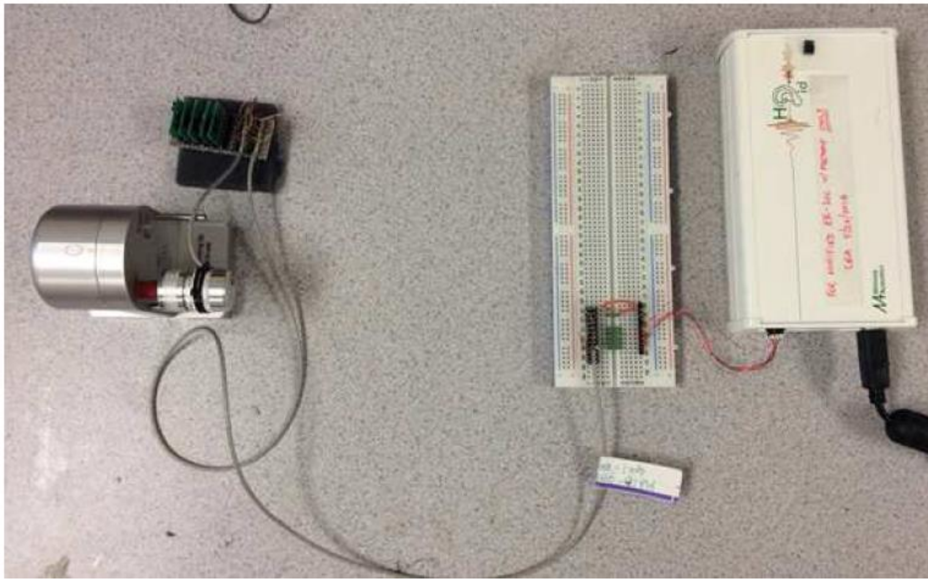

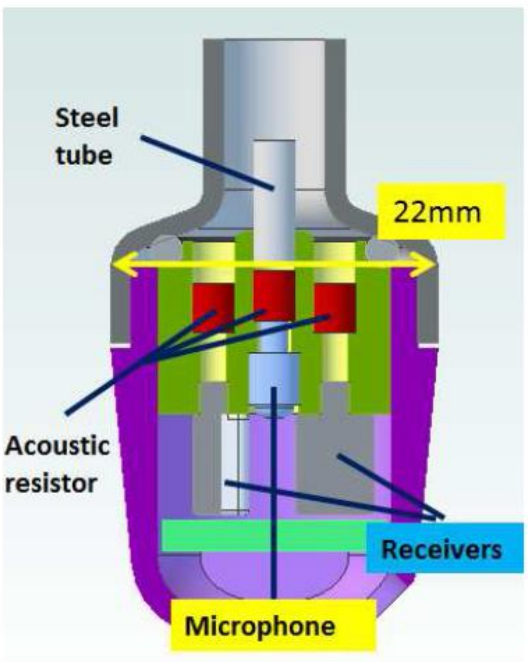

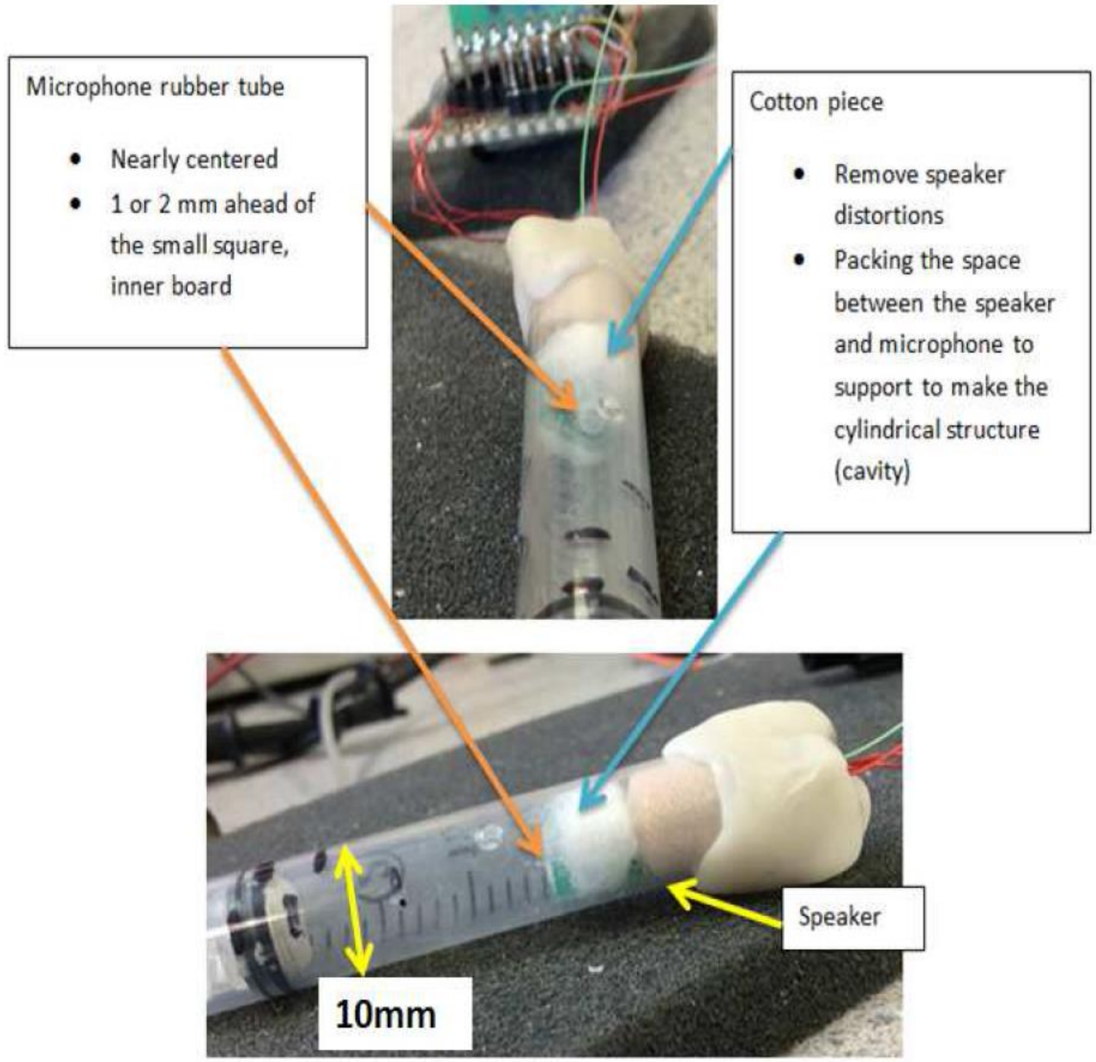

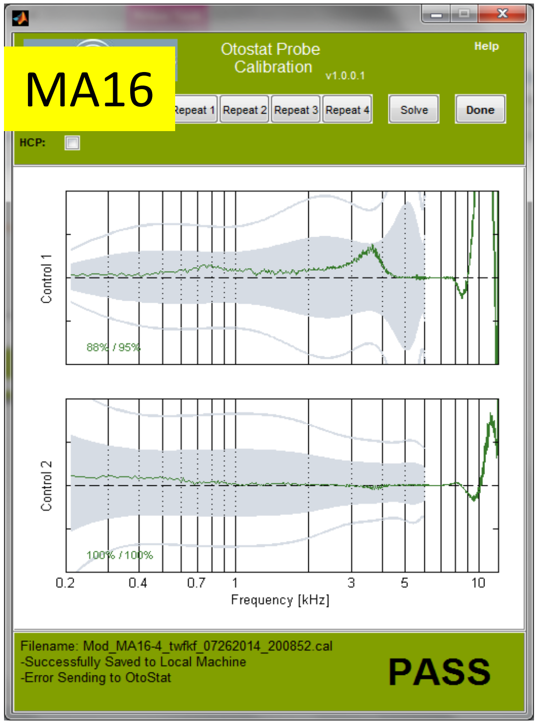

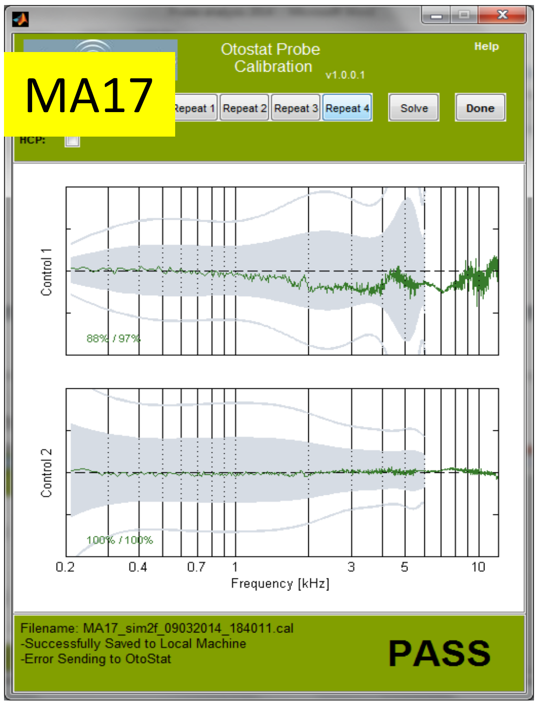

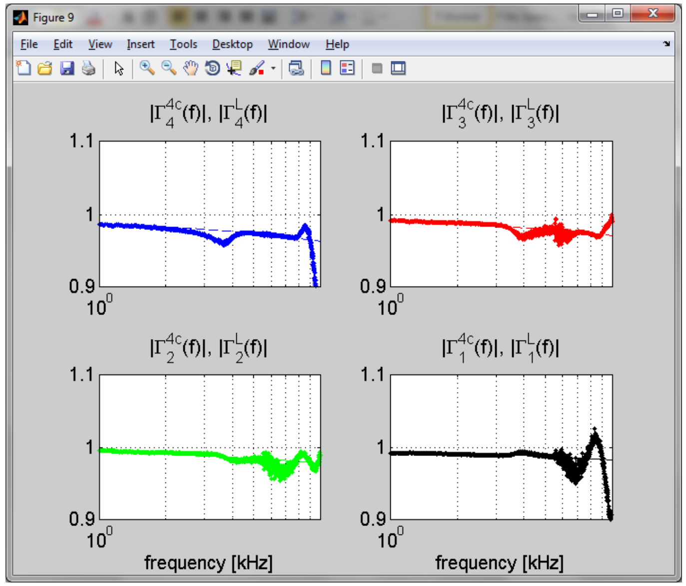

|Gamma| in each cavity

1. **Theoretical, length based:** $\Gamma_k^L = e^{-2L_k\kappa(f)}$ (dashed line)
2. **Experimental:** $\Gamma_k^{4C} = (1-Y_k^{4c})/(1+Y_k^{4c})$ (solid line) where $Y_k^{4c} = U_s/P_k - Y_s$

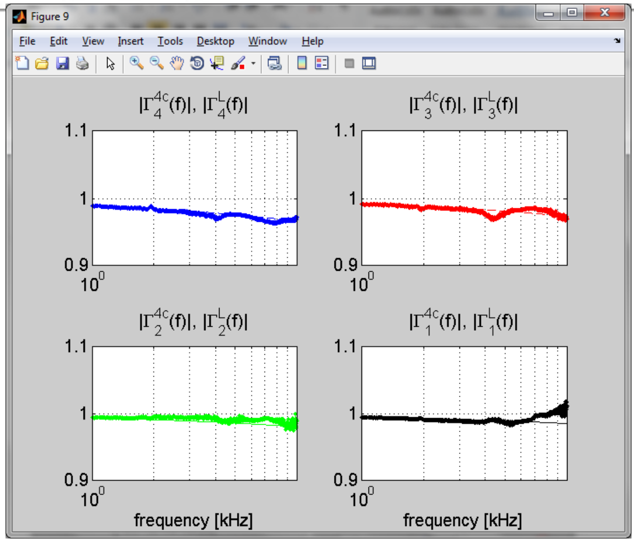

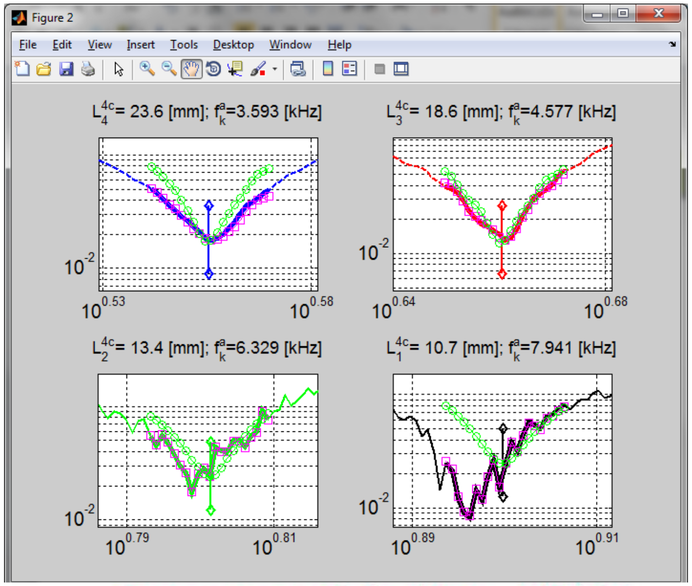

Pressure null ($c_0/4L_k \approx 45/Lk$)

1. **Theoretical (green circle):** $P_k^L = P_s/(Y_s + Y_k^L)$ where $Y_k^L = (1-\Gamma_k^L)/(1+\Gamma_k^L)$
2. **Experimental (pink circle)** $P_k^{4c} = P_s/(Y_s + Y_k^{4c})$

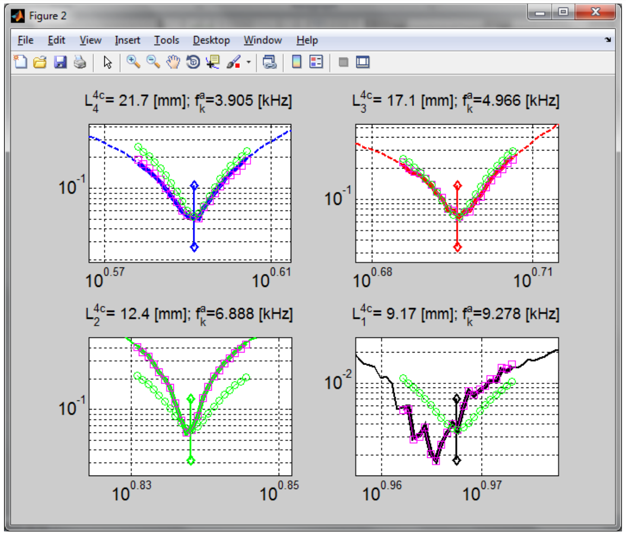

Specifications to evaluate probes

1. **Frequency responses** of both microphone and speaker should be as **flat** as possible
   - especially within the frequency range of human hearing (ideally up to 20kHz for the microphone and up to 16kHz for the speaker)
2. **Thevenin parameters** must be **stable** over time
   - This can be evaluated via source calibration (i.e., 4 cavity calibration, Allen (1986))
3. **Output levels for loudspeakers** should be **higher**
   - especially for measuring hearing impaired ears. (i.e., 85dB SPL desirable)
4. **Dynamic range** as **large** as possible
   - Dynamic range is defined as the difference between the first harmonic level and the total harmonic level at each frequency (i.e., 50-60dB is acceptable)

5. Linearity superior to current probes
   – Dynamic range should be linear across the frequency range of interest
6. Impulse response should be short and exact
   – The duration of impulse ringing should be less than 1 ms (click stimuli)
7. Crosstalk issues including all noise sources must be addressed - microphone, loudspeaker...
8. Good seal and stability in the ear canal
   – This needs good earplug design to fit a range of adult ear-canal sizes and shapes easily
9. The size of the probe is an especially critical factor in the clinic for measurements of infant ears, due to their very small ear canals.

These must take into account in the probe design !!

Conclusion II from Experimental part

- We have solved the crosstalk problem in the ER10C which has kept users from calibrating the probe above 6 kHz (can now pass 4C calibration up to 10 kHz)
- The MA16 and MA17, prototype probes, have comparable performance characteristics to the modified ER10C
- This study shows that crosstalk may be a general problem for OAE hearing probe devices which needs to be carefully addressed in the design process

CONCLUSIONS AND CONTRIBUTIONS

1. Unique BAR model
   - Extends anti-reciprocal networks using a gyrator
   - Includes a semi-inductor in the network
   - Represents non quasi-static networks by means of transmission line

2. Z_{mot} is not a physically realizable (PR) impedance
   - A simplified electro-mechanic model simulation
   - Historical background of impedance concept
     - PR property, it's not a driving point impedance

   (Physical explanation about the negative Z_{mot} real parts :Eddy-currents loss)

3. A generalization of the ABCD matrix cascading method
   - Characterized by the Möbius transformation
   - Found isomorphic relation between two methods

4. In-depth investigation of the BAR's operational principles
   – Reinterpreting the gyrator including the AC magnetic flux along with DC flux
   – Apply and investigate the classic theories to the specific BAR case, such as KCL, KVL, and the diffusion equation including the dynamic (or non-QS) terms
5. Providing essential techniques to evaluate and manufacture hearing measurement devices (in general)

Summary of contributions:

This analysis strengthens foundational knowledge of anti-reciprocal (electro-magnetic) transducer theory and application

References

Bauer, B.B., 1953. A miniature microphone for transistor amplifiers. The Journal of the Acoustical Society of America 25, 867–869.

Beranek, L.L., 1954. Acoustics. McGraw-Hill.

Beranek, L.L., Mellow, T.J., 2014. Acoustics sound fields and transducers. Waltham, MA.

Boas, R.P., 1987. Invitation to complex analysis. New York, NY.

Brune, O., 1931. Synthesis of a finite two-terminal network whose driving-point impedance is a prescribed function of frequencyg. Ph.D. thesis. Massachusetts Institute of Technology, Massachusetts.

Carlin, H.J., Giordano, A.B., 1964. Network theory, an introduction to reciprocal and nonreciprocal circuits. Englewood Cliffs NJ.

Cheng, S., Arnold, D.P., 2013. Defining the coupling coefficient for electrodynamic transducers. JASA 134(5), 3561–3672.

Fay, R.D., Hall, W.M., 1933. The determination of the acoustical output of a thelephone receiver from input measurements. Journal of Acoustic Science of America V, 46–56.

Firestone, F.A., 1938. The mobility method of computing the vibration of linear mechanical and acoustical systems. The Journal of the Acoustical Society of America 10.

Hanna, C.R., 1925. Design of telephone receivers for loud speaking purposes. Radio Engineers, Proceedings of the Institute of 13(4), 437–460.

Hunt, F.V., 1954. Electroacoustics: The analysis of transduction and its historical background. Harvard University Press. Harvard University, Massachusetts.

Jensen, J., Agerkvist, F.T., Harte, J.M., 2011. Nonlinear time-domain modeling of balanced-armature receivers. J. Audio Eng. Soc 59, 91–101.

Keefe, D.H., 1984. Acoustical wave propagation in cylindrical ducts: Transmission line parameter approximations for isothermal and nonisothermal boundary conditions. Journal of the Acoustical Society of America 75, 58–62.

Kennelly, A., 1925. The measurement of acoustic impedance with the aid of the telephone receiver. Journal of the Franklin Institute (JFI) 200, 467–487.

Kennelly, A., Affel, H., 1915. The mechanics of telephone-receiver diaphragms, as derived from their motional impedance circles. Proc. Am. Ac. Arts and Sci. 51(8), 421–482.

Kennelly, A., Kurokawa, K., 1921. Acoustic impedance and its measurement. Proc. Am. Ac. Arts and Sci. 56(1), 3–42.

Kennelly, A., Nukiyama, H., 1919. Electromagnetic theory of the telephone receiver with special reference to motional impeance. The 348th meeting of the American Institute of Electrical Engineers (A.I.E.E.) .

Kennelly, A., Pierce, G., 1912. The impedance of telephone receivers as affected by the motion of their diaphragms. Proc. Am. Ac. Arts and Sci. 48, 113–151.

Killion, M.C., 1992. Elmer Victor Carlson: A lifetime of achievement. The Bulletin of the American Auditory Society 17, 10–21.

Kim, N., Allen, J.B., 2013. Two-port network analysis and modeling of a balanced armature receiver. Hearing Research 301, 156–167.

Lin, F., Niparko, J.K., Ferrucci, L., 2011. Hearing loss prevalence in the United States. Archives of Internal Medicine 171(20), 1851–1853.

McMillan, E., 1946. Violation of the reciprocity theorem in linear passive electromechanical system. J. Acoust. Soc. Am. 18, 344–347.

Mott, E.E., Miner, R.C., 1951. The ring armature telephone receiver. The Bell System Technical Journal , 110–140.

Serwy, R., 2012. The limits of Brunes impedance. Master's thesis. University of Illinois at Urbana-Champaign, Illinois.

Tellegen, B., 1948. The gyrator, a new electric network element. Philips Res. Rep t. 3, 81–101.

Thorborg, K., Unruh, A.D., Struck, C.J., 2007. A model of loudspeaker driver impedance incorporating eddy currents in the pole structure. J. Audio Eng. Soc. .

T.S.Littler, 1934. Motional impedance diagram. Journal of Acoustic Science of America V, 235–241.

Ulaby, F.T., 2007. Fundamentals of Applied Electromagnetics, 5th ed. Prentice-Hall, Upper Saddle River, NJ.

Van Valkenburg, M.E., 1960. Introduction to Modern Network Synthesis. Wiley, NY.

Van Valkenburg, M.E., 1964. Network Analysis. Prentice-Hall, Englewood Cliffs, NJ. 2nd edition.

Vanderkooy, J., 1989. A model of loudspeaker driver impedance incorporating eddy currents in the pole structure. J. Audio Eng. Soc. 37(3), 119–128.

Warren, D.M., LoPresti, J.L., 2006. A ladder network impedance model for lossy wave phenomena. The Journal of the Acoustical Society of America (abst) 119(5), 3377.

Weece, R., Allen, J., 2010. A clinical method for calibration of bone conduction transducers to measure the mastoid impedance. Hearing Research 263, 216–223.

Wegel, R.L., 1921. Theory of magneto-mechanical systems as applied to telephone receivers and similar structures. Journal of the American Institute of Electrical Engineers 40, 791–802.

Woodson, H.H., Melcher, J.R., 1968. Electromechanical dynamics. John Wiley and Sons. New york, London, Sydney.